NRC Research Press

ARTICLE

The Road River Group of northern Yukon, Canada: early Paleozoic deep-water sedimentation within the Great American Carbonate Bank

Justin V. Strauss, Tiffani Fraser, Michael J. Melchin, Tyler J. Allen, Joseph Malinowski, Xiahong Feng, John F. Taylor, James Day, Benjamin C. Gill, and Erik A. Sperling

Abstract: Cambrian–Devonian sedimentary rocks of the northern Canadian Cordillera record both the establishment and demise of the Great American Carbonate Bank, a widespread carbonate platform system that fringed the ancestral continental margins of North America (Laurentia). Here, we present a new examination of the deep-water Road River Group of the Richardson Mountains, Yukon, Canada, which was deposited in an intra-platformal embayment or seaway within the Great American Carbonate Bank called the Richardson trough. Eleven detailed stratigraphic sections through the Road River Group along the upper canyon of the Peel River are compiled and integrated with geological mapping, facies analysis, carbonate and organic carbon isotope chemostratigraphy, and new biostratigraphic results to formalize four new formations within the type area of the Richardson Mountains (Cronin, Mount Hare, Tetlit, and Vittrekwa). We recognize nine mixed carbonate and siliciclastic deep-water facies associations in the Road River Group and propose these strata were deposited in basin-floor to slope environments. New biostratigraphic data suggest the Road River Group spans the late Cambrian (Furongian) – Middle Devonian (Eifelian), and new chemostratigraphic data record multiple global carbon isotopic events, including the late Cambrian Steptoean positive carbon isotope excursion, the Late Ordovician Guttenberg excursion, the Silurian Aeronian, Valgu, Mulde (mid-Homerian), Ireviken (early Sheinwoodian), and Lau excursions, and the Early Devonian Klonk excursion. Together, these new data not only help clarify nomenclatural debate centered around the Road River Group, but also provide critical new sedimentological, biostratigraphic, and isotopic data for these widely distributed rocks of the northern Canadian Cordillera.

Key words: Road River Group, Yukon, stratigraphy, chemostratigraphy, biostratigraphy.

Résumé : Des roches sédimentaires du Cambrien au Dévonien du nord de la Cordillère canadienne témoignent de l'établissement et de la fin du grand banc de carbonates américain, un vaste système de plateformes carbonatées qui bordait les marges continentales ancestrales de l'Amérique du Nord (Laurentie). Nous présentons les résultats d'un nouvel examen du Groupe de Road River, une unité d'eau profonde, des monts Richardson (Yukon, Canada), qui a été déposé dans un enfoncement ou un bras de mer intra-plateforme au sein du grand banc de carbonates américain appelé la fosse de Richardson. Onze coupes stratigraphiques détaillées à travers le Groupe de Road River le long du canyon supérieur de la rivière Peel sont compilées et intégrées à la cartographie géologique, l'analyse des faciès, la chimiostratigraphie des carbonates et des isotopes de carbone organique et de nouveaux résultats de biostratigraphie, permettant de définir quatre nouvelles formations dans la région type des monts Richardson (Cronin, Mount Hare, Tetlit et Vittrekwa). Nous relevons neuf associations de faciès mixtes carbonatés et silicoclastiques d'eau profonde dans le groupe de Road River et proposons que ces strates ont été déposées dans des milieux allant de fonds de bassin à des talus. De nouvelles données biostratigraphiques donnent à penser que le Groupe de Road River s'étalerait du Cambrien tardif (Furongien) au Dévonien moyen (Eifelien), et de nouvelles données chimiostratigraphiques font ressortir plusieurs épisodes d'envergure planétaire du registre des isotopes du carbone, dont l'excursion isotopique positive steptoéenne au Cambrien tardif, l'excursion de Guttenberg à l'Ordovicien tardif, les excursions aéronien, de Valgu, de Mulde (Homérien intermédiaire), d'Ireviken (Sheinwoodien précoce) et de Lau au Silurien et l'excursion de Klonk au Dévonien précoce. Collectivement, ces nouvelles données aident non seulement à éclairer des débats relatifs à la nomenclature centrés sur le Groupe de Road River, mais fournissent aussi de nouvelles données sédimentologiques, bio stratigraphiques et isotopiques clés sur ces roches largement répandues du nord de la Cordillère canadienne. [Traduit par la Rédaction]

Mots-clés : Groupe de Road River, Yukon, stratigraphie, chimiostratigraphie, biostratigraphie.

Received 25 January 2020. Accepted 7 April 2020.

J.V. Strauss, T.J. Allen, J. Malinowski, and X. Feng. Department of Earth Sciences, Dartmouth College, Hanover, NH 03755, USA.
T. Fraser. Yukon Geological Survey, Whitehorse, YT Y1A 2C6, Canada.
M.J. Melchin. Department of Earth Sciences, St. Francis Xavier University, Antigonish, NS B2G 2W5, Canada.
J.F. Taylor. Geoscience Department, Indiana University of Pennsylvania, Indiana, PA 15705, USA.
J. Day. Department of Geography, Geology, and the Environment, Illinois State University, Normal, IL 61790, USA.
B.C. Gill. Department of Geosciences, Virginia Polytechnic Institute and State University, Blacksburg, VA 24061, USA.
E.A. Sperling. Department of Geological Sciences, Stanford University, Stanford, CA 94305, USA.

Corresponding author: Justin V. Strauss (email: justin.v.strauss@dartmouth.edu).

Introduction

The early Paleozoic witnessed major evolutionary radiations and biotic crises that dramatically altered animal ecosystems (Bambach et al. 2002; Alroy et al. 2008; Servais et al. 2008; Erwin et al. 2011; Heim et al. 2015; Rasmussen et al. 2019). These significant biological events occurred against an equally profound set of global environmental changes, such as climatic shifts, changes to the redox landscape of the oceans, and major perturbations to global biogeochemical cycles (Saltzman 2005; Canfield and Farquhar 2009; Finnegan et al. 2011; Gill et al. 2011; Melchin et al. 2013; Saltzman et al. 2015). Although global in nature, many of the detailed paleontological and geochemical records that inform our knowledge of these early Paleozoic events are preserved in shallow-water mixed carbonate and siliciclastic strata of the Great American Carbonate Bank (GACB), a system of early Paleozoic sedimentary rocks deposited peripherally around the Laurentian continent (e.g., Derby et al. 2012).

The GACB was firmly established by the mid–late Cambrian, when localized thick carbonate deposits overstepped upper Ediacaran and lower–middle Cambrian rift-related successions around Laurentia. These Cambrian and Ordovician strata encompass the basal Sauk "sequence" or "megasequence" of Sloss (1963), and the broad depositional patterns and paleogeographic elements established during GACB sedimentation were commonly maintained until the late Paleozoic. In northwestern Canada, however, many Cambrian–Devonian successions continued to record localized rift-related sedimentation and complex facies changes throughout GACB sedimentation (Fritz et al. 1991; Goodfellow et al. 1995; Cecile et al. 1997; Fritz 1997; Morrow 1999; Beranek 2017; Campbell et al. 2019; Moynihan et al. 2019). A by-product of this episodic extension included the development of isolated platforms, intraplatformal sub-basins, and mixed carbonate-volcanic edifices, many of which host important economic resources (Goodfellow et al. 1995; Cecile et al. 1997; Morrow 1999; Pyle and Barnes 2003; Nelson et al. 2013; Slack et al. 2017; Johnson et al. 2018; Gadd et al. 2020). This tectonic framework of the northern Cordillera also facilitated the creation of deep-water depocenters within or directly adjacent to the GACB, many of which retain extensive, yet largely unexplored, archives of early Paleozoic Earth history. Here, we explore one of these intraplatformal deep-water basins in north-central Yukon, Canada, which is broadly referred to as the Richardson trough (Fig. 1). In addition to elucidating some of the major depositional patterns, sedimentology, biostratigraphy, and chemostratigraphy of deep-water deposits within this paleogeographic element of the GACB, we also formalize a series of new formations within the type area of the Road River Group (Road River Formation of Jackson and Lenz 1962), thereby addressing decades of nomenclatural complexity in northwestern Canada and eastern Alaska.

Geological setting

The modern mountain belts and intermontane basins of northern and central Yukon, Canada, expose a diverse early Paleozoic sedimentary succession. The main paleogeographic element that controlled depositional patterns along this part of the ancestral northwestern margin of Laurentia (in present coordinates) was a basement high called the Yukon block (Yukon stable block of Jeletzky 1962; Fig. 1). The Yukon block is defined by a region of early Paleozoic shallow-water sedimentation that was episodically isolated from the autochthonous margin of Laurentia (or Mackenzie/Peel platform) to the east by the basinal Richardson trough (Lenz 1972; Pugh 1983; Cecile et al. 1997; Norris 1997; Morrow 1999; Pyle 2012). Shallow-water early Paleozoic deposits of the Yukon block transitioned southwards into the deep-water Selwyn basin of Yukon and Northwest Territories (e.g., Lenz 1972); farther south, the Selwyn basin transitions into the Kechika trough of northern British Columbia. This isolated platform also transitioned to the north and west into Alaska and northern Yukon as deep-water continental terraces to the paleo-Pacific or Panthalassa Ocean (e.g., Payne and Allison 1981; Fritz et al. 1991; Cecile et al. 1997), but today these northwestern margins are either truncated by Mesozoic–Cenozoic faults and fold-belts or overlain by younger sedimentary deposits (e.g., Dover 1994; Norris 1997; Murphy 2018; von Gosen et al. 2019).

On the Yukon block, mixed siliciclastic and carbonate deposits of the ca. 780–540 Ma Windermere Supergroup (Strauss et al. 2015 and references therein) are regionally overlain by various unnamed Cambrian–Devonian units and shallow-water deposits of the Illtyd, Gull Lake, Slats Creek, Taiga, Bouvette, and Vunta formations, as well as the Jones Ridge Formation that straddles the Yukon–Alaska border (Morrow 1999; Dumoulin and Harris 2012; Pyle 2012; Taylor et al. 2015; Moynihan et al. 2019). These platformal rocks, as well as correlative strata of the Mackenzie/Peel and Macdonald platforms to the east and southeast (respectively), are roughly equivalent in age with deep-water carbonate and siliciclastic deposits of the Road River Group, which is locally exposed in the Richardson, Blackstone, and Kechika troughs, along with the Misty Creek embayment, Selwyn basin, and along the border with Alaska (Fig. 1; Morrow 1999; Pyle 2012 and references therein). Broadly similar platformal and basinal rocks are also exposed across the Tintina fault on the para-autochthonous Cassiar platform (or terrane) of northern British Columbia and southern Yukon (Fig. 1; Gabrielse 1963; Fritz et al. 1991; Pyle and Barnes 2000; 2001). Despite the identification of these shallow- and deep-water depocenters in the northern Cordillera, detailed correlations and stratigraphic relationships between the different facies belts, particularly within the Road River Group, are still poorly understood.

The upper(?) Cambrian to Middle Devonian Road River Group (Road River Formation of Jackson and Lenz 1962) is dominated by fine-grained carbonate and siliciclastic strata that are broadly interpreted to represent slope to basin-floor deposits (Lenz 1972; Fritz 1997; Norford 1997; Morrow 1999 and references therein). In the Richardson trough, these strata sharply to gradationally overlie either the Cambrian Illtyd or Slats Creek formations, but in other regions of Yukon, Alaska, Northwest Territories, and British Columbia they interfinger with or overlie shallow-water strata as young as Late Ordovician in age (Churkin and Brabb 1965; Brabb 1967; Blodgett et al. 1984; Fritz 1985, 1997; Rigby et al. 1988; Gordey and Anderson 1993; Cecile 2000; Pyle and Barnes 2000, 2001, 2003). Following decades of nomenclatural inconsistency, Fritz (1985) elevated the Road River "Formation" to "Group" status based on his personal observations and previous stratigraphic descriptions in the Richardson trough by Jackson and Lenz (1962) and the Selwyn basin by Cecile (1982), who distinguished Road River strata as occurring between the middle–upper Cambrian Slats Creek and Rabbitkettle formations and the overlying Middle–Upper Devonian Canol Formation.

In the Richardson Mountains, Morrow (1999) followed Fritz's (1985) treatment of the Road River strata as a group and informally subdivided the package into a basal Rabbitkettle Formation overlain by three informal shale-dominated units called the Loucheux, Dempster, and Vittrekwa formations. These new formations were guided by mapping relationships in the northern Richardson Mountains (Cecile et al. 1982) and detailed paleontological studies (particularly graptolites) of Road River Group strata in the Richardson Mountains and surrounding areas (summarized by Fritz 1997; Norford 1997; Morrow 1999; and Pyle 2012). Critically, however, these data were never incorporated into detailed sedimentological or geochemical studies. For example, the informal Road River units of Cecile et al. (1982) and Morrow (1999) were never formalized, and no type sections were assigned for these widely exposed and fossiliferous basinal strata. Furthermore, the term "Dempster" had already been used to describe Cambrian volcanic rocks of the Dawson 1:250,000 NTS map sheet (Roots 1988; Abbott

Fig. 1. (A) Paleogeographic map of the Laurentian continent (ca. 480 Ma) depicting the location of the study area (modified after Derby et al. 2012). Map created with ArcGIS. (B) Map of northern Cordilleran paleogeographic elements adapted from Pyle (2012) with main features discussed in the text. Map created with ArcGIS. (C) Simplified geologic map of the southern Richardson Mountains, Yukon, Canada. Study area outlined in boxed region (Fig. 2 map area). Base map details taken from Colpron et al. (2016) and figure generated in ArcGIS. Fm, Formation; MacD., Macdonald. [Colour online.]

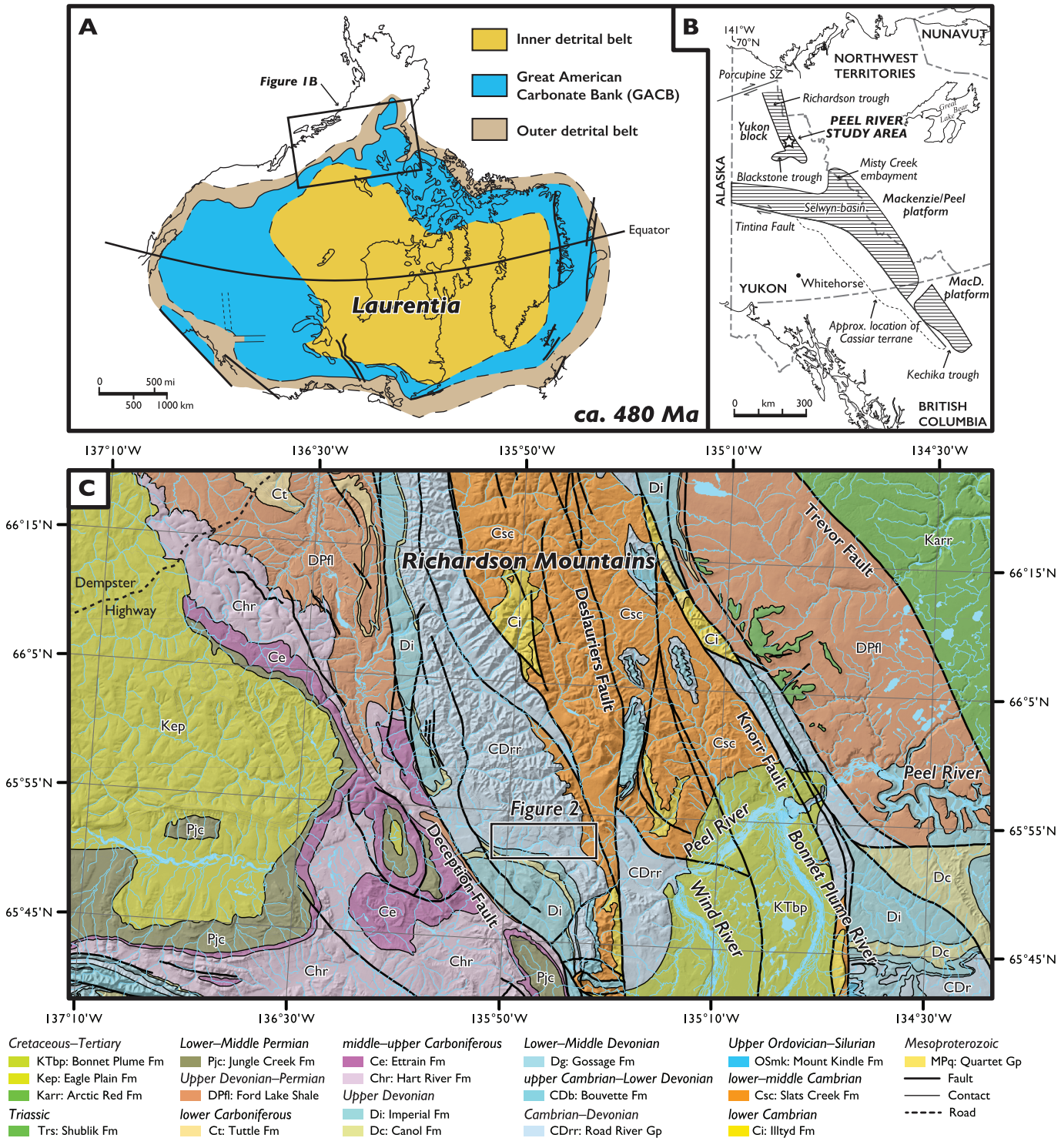

1997), and it has since been pointed out by First Nations communities that "Loucheux" is an inappropriate local term (M. Cecile, personal communication, 2020). Moreover, only one MSc thesis project focused on the sedimentology of the Road River Group (Innis 1980), and published geochemical data only came from the Ordovician–Silurian boundary interval or mineralized strata of the upper Road River Group (Hulbert et al. 1992; Goodfellow et al. 1992, 2010; Horan et al. 1994; LaPorte et al. 2009; Holmden et al. 2013; Gadd et al. 2017, 2019, 2020; Slack et al. 2017; Pages et al. 2018; Johnson et al. 2018). To address these nomenclatural issues, clarify regional

Fig. 2. Geological map of the upper canyon of the Peel River locality with location of measured sections outlined by yellow lines. Satellite image provided by the Polar Geospatial Center (© 2009 DigitalGlobe, Inc., used with permission) and base map modified from Colpron et al. (2016) in ArcGIS. [Colour online.]

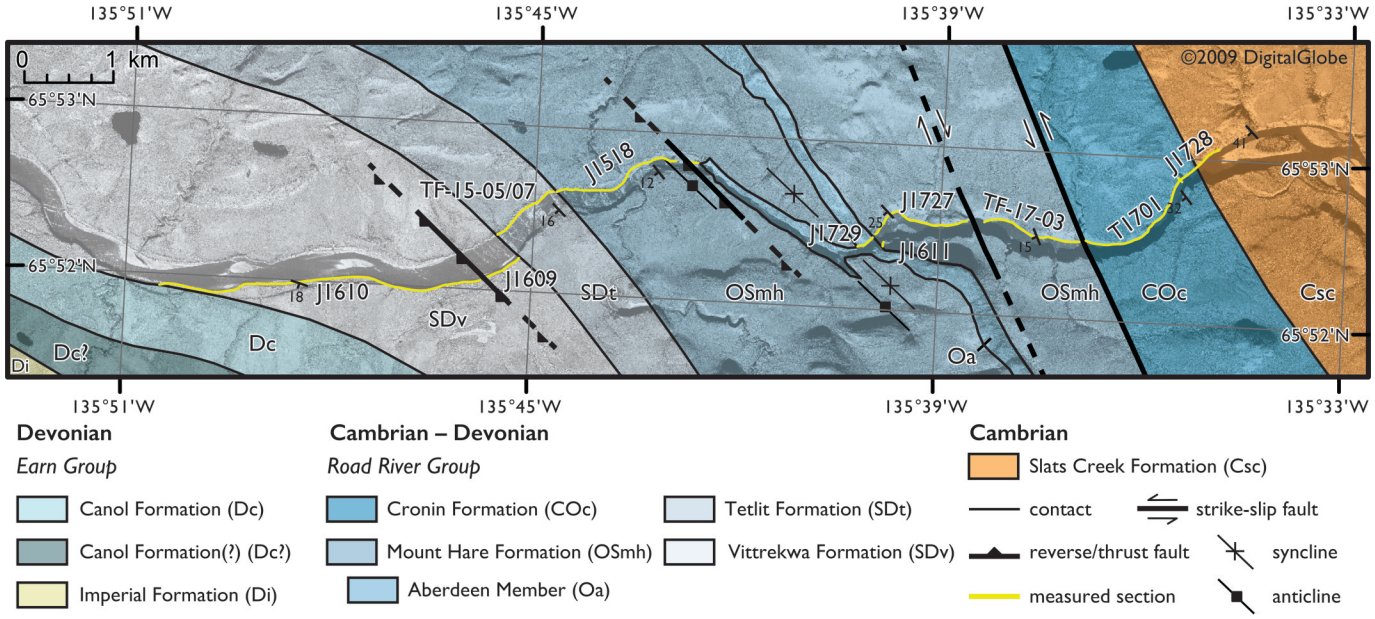

correlations, and place historical biostratigraphic collections and geochemical analyses from the Road River Group into global context, we examined well-exposed basinal rocks along the upper canyon of the Peel River in north-central Yukon (Figs. 1, 2). Here, we formalize the internal stratigraphy of the Road River Group in its type region and provide new sedimentological descriptions integrated with preliminary faunal and carbon isotope chemostratigraphic data that will pave the way for future detailed biostratigraphic and geochemical investigations.

Methods

Sedimentology and stratigraphy

Fieldwork was undertaken along the upper canyon of the Peel River over multiple two-week field seasons from 2015–2017 (Fig. 2). Eleven detailed stratigraphic sections of the Road River Group were logged at a centimetre-scale (Table 1). Owing to the inaccessibility of the entire succession from a single camp, these individual sections were combined to create a single 2472.4 m thick composite stratigraphic section that spans the entire Road River Group, along with 148.2 m of the underlying Slats Creek Formation (Fig. 3).

Stable isotope geochemistry

We present 507 new carbonate carbon ($\delta^{13}C_{carb}$) and oxygen ($\delta^{18}O_{carb}$) isotopic measurements and 674 organic carbon ($\delta^{13}C_{org}$) isotopic analyses and total organic carbon contents (TOC) from specified stratigraphic sections (all raw data are presented in Supplementary Tables S1 and S2 of the Supplementary Material[1]). Hand samples (0.1–0.5 kg) were collected at 0.5–4.0 m resolution throughout the individual measured sections for these various analyses. Isotopic results are reported in delta notation ($\delta^{13}C_{carb}$, $\delta^{18}O_{carb}$, and $\delta^{13}C_{org}$) as per mil (‰) deviations relative to the Vienna Pee Dee Belemnite (VPDB) standard. Carbonate samples were cut perpendicular to bedding and primary laminations were microdrilled (~2–10 mg of powder) to avoid secondary veins, cements, and siliciclastic components. $\delta^{13}C_{carb}$ and $\delta^{18}O_{carb}$ isotopic data were acquired on a continuous-flow Thermo Scientific (Bremen, Germany) Delta Plus XL isotope ratio mass spectrometer (IRMS) coupled with a Gasbench II (Bremen, Germany) inlet device at Dartmouth College (Hanover, New Hampshire, USA). Approximately 0.1 mg of sample powder was reacted in 12 mL glass vials with purified phosphoric acid (H_3PO_4) at 70 °C. The evolved CO_2 was analyzed against an in-house reference gas, and measured data were calibrated to the VPDB scale using three international standards (NBS–18: $\delta^{13}C_{carb}$ = –5.014‰, $\delta^{18}O_{carb}$ = –23.2; NBS–19: $\delta^{13}C_{carb}$ = +1.95‰, $\delta^{18}O_{carb}$ –2.20‰; Elemental Microanalysis – Carrera Marble: $\delta^{13}C_{carb}$ = +1.85‰, $\delta^{18}O_{carb}$ –2.22‰). Total analytical uncertainty is better than ±0.2‰ (1 standard deviation (SD)) for both $\delta^{13}C_{carb}$ and $\delta^{18}O_{carb}$ based on the repeat analysis of standards and samples.

Samples for organic carbon isotope ($\delta^{13}C_{org}$) and TOC measurements were first crushed to a flour in a tungsten carbide shatterbox vessel. The crushed powder was then decalcified either in situ in silver capsules (~2–15 mg of powder per capsule) by slowly adding drops of 1 N HCl on a hot plate or in 15 mL plastic tubes by the addition of 10 mL of 3 N HCl to ~1 g of sediment. For these latter samples, mass loss on acidification was measured and the residue was then weighed into tin capsules. Samples prepared under the first method were combusted using a Carlo Erba (Milan, Italy) NA1500 Series 2 Elemental Analyzer linked to a Thermo Scientific Delta Plus IRMS at Stanford University (Stanford, California, USA). Samples prepared under the second method were combusted in an Elementar Vario (Langenselbold, Germany) ISOTOPE cube elemental analyzer linked to an Isoprime (Manchester, UK) 100 IRMS at Virginia Tech (Blacksburg, Virginia, USA). The TOC values for the second method were then corrected to account for mass loss on acidification. At Virginia Tech, international and commercial isotopic standards (CH–6 = –10.449‰; CH–7 = –32.151‰; Elemental Microanalysis wheat flour = –27.21‰) were used to calibrate samples to the VPDB scale. Measurement of United States Geological Survey (USGS) standard SBC-1 between these two labs demonstrates comparable measurement accuracy

[1]Supplementary data are available with the article through the journal Web site at http://nrcresearchpress.com/doi/suppl/10.1139/cjes-2020-0017.

Table 1. Global positioning system coordinates (in decimal degrees) of key stratigraphic sections, Peel River, Yukon, Canada.

Sample	Section name	Map unit	Location	Latitude	Longitude
J1728	Base	Slats Creek/Rock River formations	Peel River, Richardson Mountains	65.884392	135.582850
J1728	Top	Slats Creek/Rock River formations	Peel River, Richardson Mountains	65.874512	135.614518
T1701	Base	Cronin Formation	Peel River, Richardson Mountains	65.881752	135.590261
T1701	Top	Cronin Formation	Peel River, Richardson Mountains	65.874512	135.614518
17-TF-03	Base	Mount Hare Formation	Peel River, Richardson Mountains	65.874512	135.614518
17-TF-03	Top	Mount Hare Formation	Peel River, Richardson Mountains	65.876358	135.638980
J1727	Base	Mount Hare Formation	Peel River, Richardson Mountains	65.875853	135.646407
J1727	Top	Mount Hare Formation	Peel River, Richardson Mountains	65.873555	135.667240
J1611	Base	Mount Hare Formation	Peel River, Richardson Mountains	65.873173	135.666052
J1611	Top	Mount Hare Formation	Peel River, Richardson Mountains	65.873029	135.668130
J1729	Base	Mount Hare Formation	Peel River, Richardson Mountains	65.873898	135.667378
J1729	Top	Mount Hare Formation	Peel River, Richardson Mountains	65.872632	135.669039
J1518	Base	Mount Hare Formation	Peel River, Richardson Mountains	65.880767	135.709033
J1518	Top	Mount Hare Formation	Peel River, Richardson Mountains	65.877133	135.744850
15-TF-07	Base	Tetlit Formation	Peel River, Richardson Mountains	65.877033	135.745033
15-TF-07	Top	Tetlit Formation	Peel River, Richardson Mountains	65.876483	135.764983
15-TF-05	Base	Tetlit Formation	Peel River, Richardson Mountains	65.876483	135.748317
15-TF-05	Top	Tetlit Formation	Peel River, Richardson Mountains	65.872133	135.759983
J1609	Base	Vittrekwa Formation	Peel River, Richardson Mountains	65.869714	135.754891
J1609	Top	Vittrekwa Formation	Peel River, Richardson Mountains	65.867955	135.761648
J1610	Base	Vittrekwa Formation	Peel River, Richardson Mountains	65.867730	135.763178
J1610	Top	Vittrekwa Formation	Peel River, Richardson Mountains	65.866017	135.845633

and precision (Virginia Tech: $\delta^{13}C_{org}$ = –24.49‰, SD = 0.15, TOC = 1.28 wt.%, SD = 0.08, n = 10; Stanford: $\delta^{13}C_{org}$ = –24.61‰, SD = 0.21‰, TOC = 1.28 wt.%, SD = 0.06, n = 4; USGS report TOC = 1.23 wt.% but do not report $\delta^{13}C_{org}$).

Age model construction

The age model for our composite measured section of the Road River Group (Fig. 3) was constructed by combining graptolite, conodont, brachiopod, ammonite, trilobite, and agnostoid arthropod biostratigraphic data with $\delta^{13}C_{carb}$ and $\delta^{13}C_{org}$ chemostratigraphy. The foundation of the age model for the majority of the section is from graptolite biostratigraphy (mainly planktic, graptoloid graptolites), either through new collections by our team or by placing previously published collections from the upper canyon of the Peel River in our measured sections (Lenz and Pedder 1972; Lenz 1982, 1988; Lenz and McCracken 1982; Lenz and Xu 1985; Lenz and Jackson 1986; McCracken and Lenz 1987; Jackson and Lenz 2000, 2003, 2006). Individual stratigraphic columns are provided for each section in the Supplemental Material (Supplementary Figs. S1–S9[1]); here, positive evidence for a given zone is depicted with a solid black line, whereas the stratigraphically highest sample with positive evidence for the underlying zone is represented by a dashed line. The shaded grey area between these lines thus represents stratigraphic uncertainty on the zonal boundaries; in some cases, this may be up to ~100s of m in the upper Cambrian portion of the composite section, and in other cases, it is less than the thickness of the solid line in the supplemental figures[1].

The dominantly unfossiliferous upper Cambrian portion of the composite section (measured sections J1728 and T1701; Supplementary Figs. S1–S2[1]) was assigned to the Furongian Series on the occurrence of a diagnostic, basal Furongian agnostoid arthropod species near the base of the Cronin Formation and distinctive features of the $\delta^{13}C_{carb}$ profile near the base of the Mount Hare Formation that strongly resemble the pattern documented through the Cambrian–Ordovician boundary interval elsewhere (see below). Although the analysis of taxa present in six new conodont collections from the Cronin Formation is not yet complete, preliminary identifications suggest that all are Furongian in age (Supplemental Material[1]; Nowlan 2019). For the Ordovician through Llandovery it is possible to define individual graptolite zones, but graptolites are relatively rare in the Wenlock, Ludlow, and Pridoli (a pattern seen throughout the Richardson trough by Lenz 1972, 1978) where individual zones cannot be defined. Rather, age boundaries in this part of the section are drawn based on the graptolites that were found plus the identification of diagnostic positive $\delta^{13}C_{org}$ excursions (Fig. 3). Graptolites are more common throughout the Lower Devonian strata, and diagnostic Middle Devonian (*Polygnathus eiflius* to *Polygnathus ansatus* Zone) conodonts were found at the top of the composite section in a thin, mineralized interval beneath the overlying Canol Formation (Gadd et al. 2020). Given the remote location of our study area and the fact that parts of our age model are based on correlation with collections made nearly 50 years ago, we have elected to include some verbatim notes from one of the authors (M.J. Melchin) in the Supplemental Material[1] – we believe these will be of high utility to future researchers interested in revisiting this locality.

Results

Stratigraphy

The Road River Group is divided here into four new formations (Cronin, Mount Hare, Tetlit, and Vittrekwa) that can be correlated at map scale throughout the Richardson Mountains (Cecile et al. 1982; M. Cecile, personal communication, 2020), and perhaps even into other regions of Yukon, Northwest Territories, and British Columbia, Canada, and Alaska, USA (e.g., Jackson and Lenz 1962; Fritz 1985; Morrow 1999; Pyle 2012). Below, we present tables that detail the key lithostratigraphic characteristics of each new Formation (Tables 2, 3, 4, 5) and provide a brief overview of the major contacts and distinguishing characteristics of each unit within the main text. The exposures along the upper canyon of the Peel River described in this study are here designated as the type section for all four of these formations (Fig. 2).

The Cronin Formation (Table 2) comprises 948 m of dark- to medium-grey lime mudstone, wackestone, and grainstone interbedded with black calcareous to silicified shale and minor chert (Figs. 3; Supplementary Figs. S1, S2[1]). These strata are notably resistant compared with bounding strata of the Slats Creek and Mount Hare formations due to the predominance of carbonate lithofacies in this unit (Figs. 4A, 4B). At the upper canyon of the Peel River locality, the Cronin Formation conformably and gradationally overlies interbedded dark grey to brown shale, siltstone, and sandstone of the Slats Creek Formation, and its base is de-

Fig. 3. Composite measured stratigraphic section of the Road River Group, Peel River, Yukon, Canada. Lines between Silurian chronostratigraphic units are dashed due to uncertainty of placement within measured section. Individual measured sections are provided in the Supplemental Material[1]. Carbon isotopes are plotted against separate scales for $\delta^{13}C_{carb}$ (bottom) and $\delta^{13}C_{org}$ (top). A., Aberdeen Member; Aer., Aeronian; Darriwil., Darriwilian; E.–G., Eifelian–Givetian; Em., Emsian; ESCIE, early Sheinwoodian carbon isotope excursion; G.?, Gorstian?; GICE, Guttenberg Excursion; Hom., Homerian; Kat., Katian; L., Lochkovian; Ludford., Ludfordian; Pra., Pragian; Prid., Pridoli; Rhu., Rhuddhanian; S., Sandbian; Shein., Sheinwoodian; SPICE, Steptoean positive carbon isotope excursion; TR, Tremadocian Stage; Wen., Wenlock. [Colour online.]

fined by the first appearance of interbedded limestone and shale (Figs. 3, 4C; Supplementary Fig. S1[1]). The upper contact with the Mount Hare Formation is locally truncated by a dextral strike-slip fault in our field area (Figs. 2, 3); however, this contact is gradational in other localities in the Richardson Mountains, where it is marked by a sharp decrease in the overall proportion of lime mudstone (Cecile et al. 1982).

The 748.2 m thick Mount Hare Formation (Table 3) consists of a diverse assemblage of interbedded light grey to black shale, limestone, and chert with rare matrix- or clast-supported carbonate rudstone, breccia, megabreccia and tephra horizons (Figs. 3; Supplementary Figs. S3–S6[1]). These dominantly fine-grained strata are locally deformed by minor faults and folds in the field area (Figs. 2, 3, 5A–5C), all of which were traced and accounted for in our detailed measured sections. The Mount Hare Formation contains a distinct 26.9 m thick unit dominated by very thick-bedded matrix-supported rudstone, breccia, and megabreccia that we distinguish herein as the Aberdeen Member (Figs. 2, 3, 5, 6; Supplementary Fig. S5[1]). The upper contact of the Mount Hare Formation is marked by a sharp transition from recessive black graptolitic shale to resistant orange-weathering dolosiltite and dolograinstone of the overlying Tetlit Formation (Figs. 3, 7A).

The 215.5 m thick Tetlit Formation (Table 4) is characterized by multiple decametre-thick packages of alternating recessive grey-black calcareous shale and resistant interbedded orange-weathering dolosiltite, dolograinstone, calcareous shale/mudstone, and matrix- to clast-supported rudstone, packstone, and grainstone (Figs. 3, 7; Supplementary Fig. S7[1]). These strata are overlain conformably by the 412.5 m thick Vittrekwa Formation (Table 5), the basal contact of which is marked by a conformable transition to interbedded calcareous shale and lime mudstone (Fig. 3; Supplementary Fig. S8[1]). The Vittrekwa Formation is dominated by dark grey to black interbedded calcareous and pyritic shale, calcisiltite, and lime mudstone with rare thin beds of fossiliferous grainstone or wackestone (Figs. 3, 8; Supplementary Figs. S8–S9[1]). These strata become more silicified up-section below a sharp paraconformable contact with the overlying Canol Formation of the Earn Group (Figs. 3, 8B). The uppermost metre of the Vittrekwa Formation contains a regionally persistent and centimetre-scale hyper-enriched black shale Ni–Mo–Zn–Pt–Pd–Au–Re deposit (Gadd et al. 2020), locally referred to as the Nick horizon (Goodfellow et al. 1992), which overlies distinctive and regionally persistent metre-scale carbonate concretions.

Facies associations

Nine facies associations (FAs) have been recognized here in the Road River Group along the upper canyon of the Peel River (Table 6). In Table 6, and in the following Discussion, turbidite structures (T_{A-E}) are given according to standard Bouma subdivisions (Bouma 1962) and the term "megabreccia" follows Spence and Tucker (1997).

Facies associations 1, 2, 3, and 4

The Road River Group is dominated by very fine-grained siliciclastic and carbonate lithofacies of FAs 1–4 (Fig. 3; Supplementary Figs. S1–S9[1]; Table 6). These strata are characterized by structureless to well-laminated interbedded shale, mudstone, chert, lime mudstone, and calcisiltite with rare normal graded to massive, very thin to thin beds of fossiliferous wackestone, packstone, or grainstone (commonly <5%; Fig. 8D). Mudrocks of FAs 1–4 are commonly dark grey to black with TOC contents ranging from 0.15%–8.78%, although lime mudstone units of FA 4 locally weather light grey to white (Figs. 5, 7, 8). All of these FAs are locally graptolitic (Fig. 3), and some of them preserve intervals of sparse to heavy bioturbation (Figs. 7G, 8H). Bedding bounding surfaces in FAs 1–4 are commonly planar to undulatory with occasional scour horizons, slump folds (Figs. 5D–5F, 7C), synsedimentary truncation surfaces (Fig. 8C), soft-sediment deformation structures (Fig. 7E), and centimetre- to metre-scale concretionary intervals (Fig. 8E).

Facies association 5

Facies association 5 only occurs in the Tetlit Formation and consists of moderately resistant buff- to orange-weathering calcisiltite, dolosiltite, and argillaceous dolograinstone (Figs. 3, 7). These strata are commonly medium- to thick-bedded, planar to ripple cross-laminated, and display planar to undulatory bounding surfaces with occasional normal grading (Figs. 7B, 7F). Some of these beds are transitional from centimetre-thick basal matrix-supported fossiliferous rudstone, grainstone, and packstone horizons (Fig. 7D), whereas other packages overlie intervals of FAs 1–4 that display slump folds and (or) chaotic internal soft-sediment deformation (Figs. 7C, 7E). Bioturbation and localized silicification is common throughout this FA (Fig. 7G).

Facies associations 6 and 7

Carbonate-dominated strata of FAs 6 and 7 characterize the entirety of the Cronin Formation and form discrete resistant intervals in the Vittrekwa Formation (Fig. 3). These strata consist of blueish- to dark-grey lime mudstone, calcisiltite, and minor wackestone, packstone, and grainstone interbedded with black calcareous shale and mudstone (Figs. 4B, 4D). Bedding in these FAs ranges from very thin to thick with mostly planar to undulatory bounding surfaces, the latter of which are generally erosive into underlying finer-grained intervals (Fig. 4E). Some strata in FA 6 display very thin to thin "ribbon" textures with <5 cm thick shale or mudstone partings. These FAs are commonly massive or display planar lamination, although some beds in FA 7 display ripple- to dune-scale cross-stratification, normal grading, and soft-sediment deformation. Slump folding is present in both FAs 6 and 7 (Fig. 4F), as are thin pyritic fossiliferous lags dominated by inarticulate and articulate brachiopod debris (Fig. 4E). Benthic graptolites, trilobites, agnostoid arthropods, and tephra horizons are present but rare in the Cronin Formation (Figs. 3, 4G, 4H), whereas centimetre- to metre-scale black chert nodules and complete chert replacement are present throughout both of these FAs.

Facies associations 8 and 9

Prominent white to dark-grey clast- and matrix-supported rudstone, breccia, and megabreccia characterize FAs 8 and 9 and commonly form marker beds throughout the Road River Group (Fig. 3; Cecile et al. 1982). Pebble- to boulder-clast rudstone and breccia horizons up to ~4 m thick are present in the Mount Hare and Tetlit formations, whereas the boulder rudstone and megabreccia horizons of FA 9 are only present in the Aberdeen Member of the Mount Hare Formation. Both of these FAs are commonly poorly sorted and stratiform in geometry with sharp basal contacts (Figs. 5C, 6B); finer-grained strata beneath these horizons occasionally display internal deformation (Fig. 6C). Clasts within these coarse-grained facies are commonly angular to sub-rounded

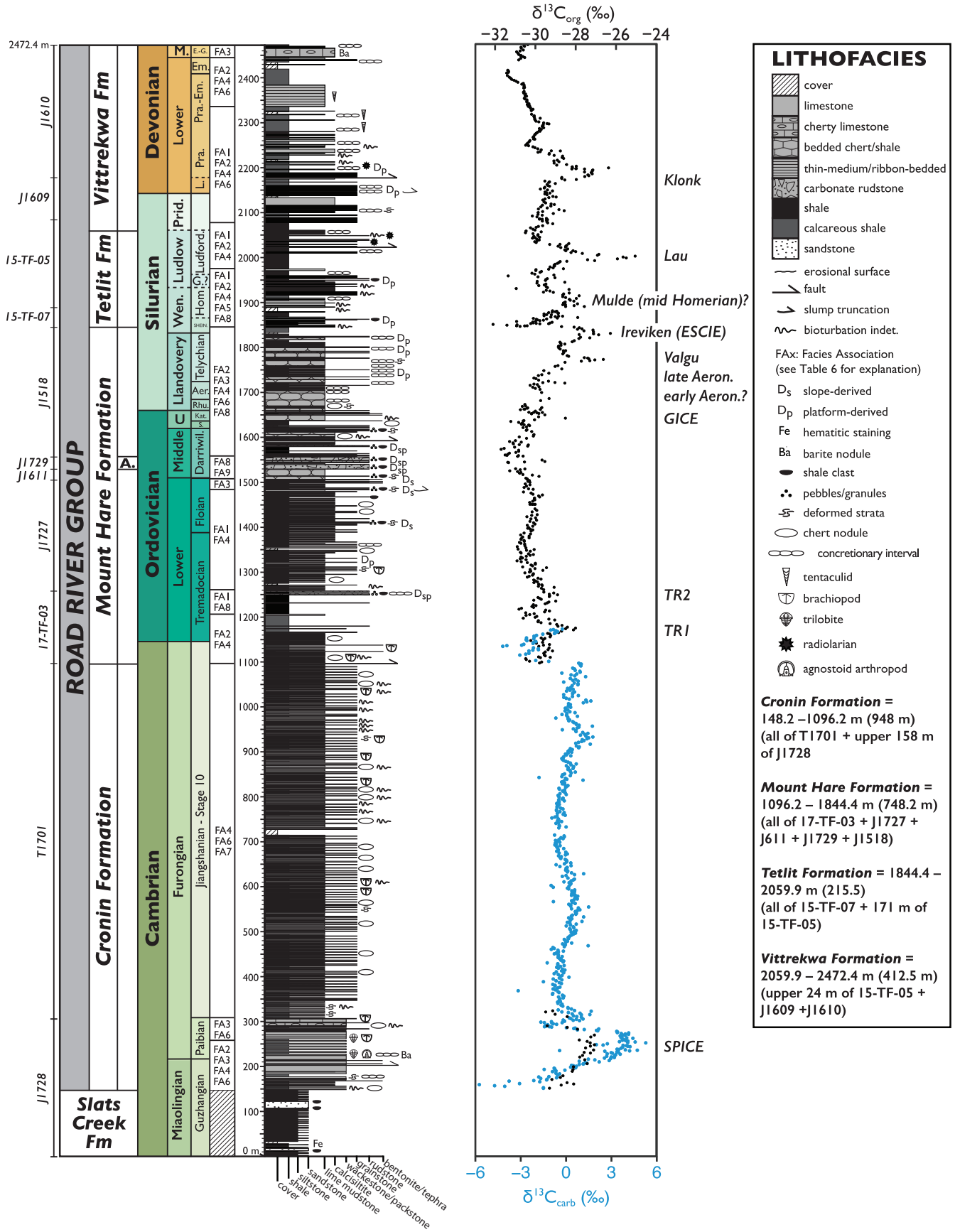

Table 2. Formalization of the Cronin Formation, Road River Group.

Name	Cronin Formation
Name derivation	Named after Mount Cronin within the Richardson Mountains, Yukon Territory, Canada; Eagle River Quadrangle (NTS 116I); M. Cecile, personal communication, 2020
Category and rank	Lithostratigraphic Formation
Type area	Exposures along the Peel River, southwestern Richardson Mountains, Yukon Territory, Canada
Unit type section	Section J1728–T1701 (Fig. 3; this paper) Located on north side of Peel River about 4–5 km downstream from Aberdeen Canyon Lower boundary: gradational contact with interbedded shale, siltstone, and sandstone of Slats Creek Formation (65.882946, 135.586117) Upper boundary: faulted contact with Mount Hare Formation (65.874512, 135.614517)
Historical nomenclature	Previously referred to as map unit CDrl of Norris (1981*a*, 1981*b*, and 1981*c*), COr of Cecile et al. (1982), or the "Rabbittkettle Formation" of Morrow (1999)
Unit description	Generally monotonous succession of bioturbated resistant argillaceous limestone exposed throughout the Richardson Mountains. Basal contact with underlying strata of the Slats Creek Formation (previously called map unit CDr0 of Norris (1981*a*, 1981*b*, and 1981*c*) or Csh of Cecile et al. (1982)) is gradational with contact defined as first appearance of interbedded limestone. The basal 20.6 m is dominated by interbedded black calcareous shale, chert, and dark grey and variably silicified lime mudstone with rare fine-grained fossiliferous wackestone and pyritic bentonite horizons. Overlying 123 m composed of thin- to medium-bedded lime mudstone, calcisiltite, wackestone, and grainstone with large variety of Bouma subdivisions, variable silicification, concretionary intervals, slump folds, barite nodules, nodular chert, and rare fossiliferous intervals with benthic graptolites and disarticulated phosphatic and calcareous brachiopods and trilobites. These strata are overlain by 16 m of thin- to medium-bedded calcareous turbidites with Bouma $T_{A–E}$ subdivisions and fossiliferous basal grainstones lags. The overlying 790 m of the Cronin Formation is dominated by a monotonous succession of medium-bedded lime mudstone, wackestone, and minor grainstone with rare intervals of thin or thick bedding and basal fossiliferous lags comprised of disarticulated brachiopod valves. These strata contain numerous intervals with slump folds, silicification, and stratiform concretionary zones. The upper contact with the Mount Hare Formation is truncated by a dextral strike-slip fault on the Peel River.
Unit reference section	Reported but incomplete ~1910 m exposure along Rock River, Richardson Mountains, Yukon (M. Cecile personal communication in Morrow 1999) Coordinates for reference "Section 3" of Morrow (1999) is at 66°45′45″N, 136°19′W
Dimensions	948 m thick at type section (Fig. 3, this paper); ~1910 m thick at reference section
Geologic age	Cambrian (Furongian Series, Paibian–Stage 10; this paper)
Regional correlations (shelf)	Jones Ridge, Bouvette, Taiga, and Franklin Mountain formations of Alaska, USA, and Yukon, and Northwest Territories, Canada
Regional correlations (slope/basin)	Hillard, Rabbitkettle, Broken Skull, and Kechika formations of Alaska, USA, and Yukon, and Northwest Territories, Canada

and range from pebble to raft in size (Figs. 6B–6H). The clast compositions are variable, with some beds being dominated by reworked strata from FAs 1–7 (Fig. 5H) and others comprising allochthonous shallow-water material consisting of oolitic and pisolitic dolograinstone, fragmented or whole fossil debris, microbial boundstone with *Epiphyton* and *Renalcis*, fossiliferous reefal boundstone/framestone, sandy dolostone, and silicified breccia (Figs. 6C–6H). The Aberdeen Member locally contains decametre-scale rafts of interbedded shale, mudstone, and lime mudstone of FAs 1–4 (Fig. 6E), as well as blocks of fossiliferous wackestone and boundstone with quartz sand-filled grikes and silicified breccia (Figs. 6F, 6G). The irregular upper surfaces of beds within FAs 8 and 9 are commonly draped by finer-grained strata of FAs 1–4 (Fig. 6H).

Biostratigraphy

Glyptagnostus reticulatus, an agnostoid arthropod whose first appearance datum defines the base of the Cambrian Furongian Series and Paibian Stage (Peng et al. 2004), was discovered at 217.5 m in section J1728 of the Cronin Formation (Figs. 4G, 4H; Supplementary Fig. S1[1]), providing a firm basal age constraint on the lower Road River Group at the upper canyon locality. Collections of conodonts with conodont alteration index (CAI) values ranging from 2–3 were recovered at six horizons (335.55 m, 386.63 m, 514.11 m, 568.49 m, 662 m, 680 m, and 703 m) in section T1701 of the Cronin Formation (Supplemental Material, Supplementary Fig. S2[1]; Nowlan 2019). Preliminary identifications from these collections suggests that the represented taxa include *Phakelodus?* sp., several species of *Proconodontus* Miller, 1969, *Cordylodus proavus* Müller, 1959, and *Teridontus* sp. No attempt was made to place the boundary between Stage 10 and the underlying Jiangshanian Stage in Fig. 3, in part because of the preliminary nature of the conodont identifications, but also because deliberations regarding the biostratigraphic horizon to be used to define that boundary are still ongoing (e.g., Miller 2019).

A number of other conodont collections from sections J1518, TF-17-05, and TF-17-07 of the Mount Hare Formation yielded sparse, yet diverse, conodont elements with CAI values ranging from 4–6 (Supplemental Material[1]). These collections are consistent with bounding graptolite biostratigraphic data, so they are not discussed further. However, one collection from an allochthonous microbial boundstone raft within the Middle Ordovician (Darriwilian) Aberdeen Member (sample J1519) yielded late Early Ordovician (Floian Series) specimens of *Bergstroemognathus extensus*, *Juanognathus variabilis*, and *Periodon* sp., confirming reworking of older Lower Ordovician strata within the Aberdeen Member.

In the uppermost exposures of the Road River Group, abundant brachiopods at 12.9 m in section J1610 of the Vittrekwa Formation are referred to *Ogilviella* sp. cf. *Ogilviella canadensis* Smith, 1980, which likely represents an early Lochkovian age (Early Devonian), although the genus ranges from Pridoli to Lochkovian. A specimen of *Protocortezorthis* sp. was also collected in section J1610 from 150.5–151.5 m, which indicates a late Lochkovian or early Pragian age (Early Devonian), and a goniatite collected at 261 m was identified as *Agoniatites*, suggesting an Eifelian–Givetian (Middle

Table 3. Formalization of the Mount Hare Formation, Road River Group.

Name	Mount Hare Formation
Name derivation	Named after Mount Hare within the western Richardson Mountains, Yukon Territory, Canada; Eagle River Quadrangle (NTS 116I); M. Cecile, personal communication, 2020
Category and rank	Lithostratigraphic Formation
Type area	Exposures along the Peel River, southwestern Richardson Mountains, Yukon Territory, Canada
Unit type section	Sections 17-TF-03–J1727-J1611-J1729-J1518 (Fig. 3; this paper) Located on north side of Peel River spanning 2–3 km upstream and downstream of Aberdeen Canyon, Yukon Territory, Canada Lower boundary: faulted contact with upper Cronin Formation in prominent north-trending drainage (65.874512, 135.614517) Upper boundary: Sharp contact with basal fine-grained orange-weathering dolosiltites of the Tetlit Formation (65.877133, 135.74485)
Historical nomenclature	Previously referred to as upper part of map unit CDrl of Norris (1981*a*, 1981*b*, and 1981*c*), unit OSl of Cecile et al. (1982), and the "Loucheux Formation" of Morrow (1999)
Unit description	Variable succession of black shale, siliceous shale/siltstone, chert, and argillaceous limestone exposed throughout the Richardson Mountains. Basal contact with underlying strata of the Cronin Formation is faulted at type section but regionally is gradational and marked by an increase in shale content. Basal 62 m is dominated by interbedded dark grey to black pyritic calcareous black shale, argillaceous to silicified limestone, chert, and minor grainstone, wackestone, and matrix-supported rudstone. Strata are locally bioturbated and/or graptolitic and contain rare tephra horizons, fossiliferous grainstone or wackestone lenses, soft-sediment deformation, slump folds, and concretionary intervals. These strata are overlain by 100 m of recessive black calcareous and pyritic shale with abundant nodular pyrite concretions and rare graptolites, which are capped by two prominent ~2 m thick carbonate rudstone horizons. These marker beds enable tracing of these strata across a small strike-slip fault and through a broad fold, where they transition into 270 m of interbedded graptolitic black shale, calcareous shale, and dark to light grey lime mudstone, calcisiltite, and fine-grained grainstone. These strata are fine- to medium-bedded and contain remarkably consistent Bouma $T_{ABE–ABCE}$ subdivisions, as well as local slump folds, synsedimentary truncation surfaces, concretionary intervals, chert nodules, and fossiliferous grainstone horizons with shelf-derived corals, gastropods, crinoids, and brachiopod debris. These strata are overlain by 24 m of interbedded graptolitic silicified black shale and chert with rare bentonite horizons, fossiliferous wackestone or packstone lenses, and carbonate rudstone horizons with planar basal contacts. This highly silicified interval is overlain by the Aberdeen Member, which consists of two >6 m thick amalgamated carbonate rudstone to megabreccia horizons with abundant shelf- and slope-derived clasts and rafts, planar to erosional bases, and discontinuous intervals of black graptolitic shale and calcareous shale. The Aberdeen Member is overlain by 270 m of interbedded black graptolitic calcareous and silicified shale, chert, and minor silicified lime mudstone, wackestone, and grainstone with local bioturbation, slump folds, synsedimentary truncation surfaces, tephra horizons, and silicified carbonate rudstone with shelf- and slope-derived clasts. Locally, these strata contain prominent concretionary intervals that appear to nucleate on porous carbonate rudstone horizons or chaotic slump-folded intervals. In the upper 75 m, these strata host abundant pyritized and silicified fossiliferous rudstone, grainstone, and wackestone horizons with tabulate and rugose corals, nautiloids, gastropods, brachiopods, and crinoids. The upper 20 m of this unit is poorly exposed and consists of recessive black graptolitic and pyritic calcareous shale that is abruptly overlain by resistant strata of the Tetlit Formation.
Unit reference section	Reported but unmeasured ~525 m exposure along Trail River, Richardson Mountains (M. Cecile personal communication in Morrow 1999)
Dimensions	748.2 m thick at type section (Fig. 3, this paper); ~525 m thick at reference section
Geologic age	Cambrian–Silurian (Furongian Series, Stage 10–Wenlock, Sheinwoodian; this paper)
Regional correlations (shelf)	Jones Ridge, Bouvette, Franklin Mountain, Mount Kindle, Beaverfoot, and Skoki formations of Alaska, USA, and Yukon, and Northwest Territories, Canada
Regional correlations (slope/basin)	Duo Lake, Haywire, Marmot, Ospika, Robb, Whittaker, Esbataottine, and Sunblood formations of Alaska, USA, and Yukon, and Northwest Territories, Canada

Devonian) age (R.B. Blodgett, personal communication, 2017). Conodonts with CAI values ranging from 3–4 were recovered 1.08 m below the top of section J1610 (and the Nick horizon; Supplementary Fig. S9[1]), which provides a *Polygnathus eiflius* – *Polygnathus ansatus* Zone age (late Eifelian – middle Givetian, Middle Devonian) and confirms a recent 387.5 ± 4.4 Ma Re–Os geochronological age from the host strata (Gadd et al. 2020).

Stable isotope geochemistry

New $\delta^{13}C_{carb}$ and $\delta^{18}O_{carb}$ measurements from the carbonate-dominated Cronin Formation range from –5.7 to +5.3‰ and –13.7 to –6.7‰, respectively (Fig. 3; Supplementary Figs. S1–S3[1]). Our composite measured section starts with depleted $\delta^{13}C_{carb}$ values and displays a prominent positive excursion with peak values reaching +5‰. This positive spike is followed by a short-lived negative excursion down to –1.6‰, followed by another positive excursion to +1.7‰ before returning to a baseline of oscillating values between –1‰ and +1‰. Around ~850 m in the composite section, the $\delta^{13}C_{carb}$ values start to trend towards more enriched compositions and record two abrupt positive excursions to +1.5‰ (Fig. 3). This is followed by a prominent negative shift in $\delta^{13}C_{carb}$ values down to –4.2‰ across the fault at the Cronin – Mount Hare Formation boundary, which transitions up-section into more enriched values of –0.25‰ in the basal Mount Hare Formation (Supplementary Fig. S3[1]). $\delta^{18}O_{carb}$ data from the Cronin Formation are consistent throughout the unit, with small-scale (<1‰) oscillations around a mean of –9‰ (Supplementary Table S1[1]).

Organic carbon isotopic data ($\delta^{13}C_{org}$) from the Road River Group range from –25.0‰ to –32.1‰ and record a number of

Table 4. Formalization of the Tetlit Formation, Road River Group.

Name	Tetlit Formation
Name derivation	Named after Tetlit Creek within the eastern Richardson Mountains, Yukon Territory, Canada; Trail River Quadrangle (NTS 106 L)
Category and rank	Lithostratigraphic Formation
Type area	Exposures along the Peel River, southwestern Richardson Mountains, Yukon Territory, Canada
Unit type section	Sections 15-TF-05 and 15-TF-07 (Fig. 3; this paper) Located on north side of Peel River ~1–2 km upstream of Aberdeen Canyon, Yukon Territory, Canada Lower boundary: abrupt contact with calcareous shale of the upper Mount Hare Formation (65.877133, 135.74485) Upper boundary: Gradational contact with black calcareous shale and limestone of the Vittrekwa Formation (65.872833, 135.7577)
Historical nomenclature	Previously referred to as upper part of map unit CDr3 of Norris (1981*a*, 1981*b*, and 1981*c*), unit Sd of Cecile et al. (1982), and the "Dempster Formation" of Morrow (1999)
Unit description	Variable succession of black shale, siliceous and calcareous shale/siltstone, argillaceous and dolomitic limestone, and minor chert exposed throughout the Richardson Mountains. Basal contact with underlying strata of the Mount Hare Formation is marked by an abrupt transition from recessive, calcareous black shale of the upper Mount Hare Formation into resistant orange-yellow-weathering dolosiltite and very-fine-grained dolograinstone of the basal Tetlit Formation. Lower 25 m dominated by interbedded orange-yellow-weathering dolosiltite and fine-grained dolograinstone, black to dark grey shale and calcareous shale, dark grey to brown silicified lime mudstone and calcisiltite, and fossiliferous carbonate rudstone and wackestone. Bioturbation, slump folds, synsedimentary truncation surfaces, and distinct Bouma T_{ABCDE} subdivisions are present throughout this interval with the orange-weathering dolomitic beds forming prominent cliffs dominated by medium to thick bedding. These strata are overlain by 20 m of poorly exposed and recessive calcareous black shale and then a second 15 m thick cliff-forming orange-weathering dolosiltite and very-fine-grained dolograinstone succession with local fossiliferous and bioturbated intervals. The overlying 55 m of the Tetlit Formation is dominated by interbedded calcareous and graptolitic shale, calcisiltite, very fine- to coarse-grained grainstone, wackestone, and minor carbonate rudstone. These heterogeneous strata contain Bouma T_{ABCE} subdivisions, channelized horizons, slump folds, erosional scours with shale rip-up clasts, shelf- and slope-derived matrix-supported rudstones, and local evidence for bioturbation and prominent concretionary intervals. This unit is overlain by 100 m of fine-grained strata dominated by black shale that is variably calcareous and silicified, with occasional intervals of thin-bedded calcisiltite and very-fine-grained grainstone, fossiliferous rudstone and wackestone, and concretionary intervals that are nucleated on coarse-grained lithofacies. The contact with the overlying Vittrekwa Formation is a gradational transition into calcareous shale and mudstone that is locally marked by a prominent concretionary interval.
Unit reference section	Reported as ~100–144 m from exposures along Rock and Trail rivers, Richardson Mountains (M. Cecile personal communication in Morrow 1999)
Dimensions	215.5 m thick at type section (Fig. 3, this paper); ~100–144 m thick at reference sections
Geologic age	Silurian (Wenlock, Sheinwoodian–Pridoli(?); this paper)
Regional correlations shelf)	Mount Kindle, Whittaker, Nonda, Kwadacha, Muncho, McConnell, and Ramhorn formations of Yukon and Northwest Territories, Canada
Regional correlations (slope/basin)	Steele, Duo Lakes, and Esbatoattine formations of Yukon and Northwest Territories, Canada

prominent excursions (Fig. 3; Supplementary Figs. S1–S9[1]; Supplemental Material[1]). $\delta^{13}C_{org}$ data from the basal Cronin Formation start at –29.3‰ and record a prominent positive excursion to –27.1‰ before recovering to the pre-excursion values. The remainder of the Cronin Formation was not analyzed for organic carbon isotopes. The Ordovician portion of the Mount Hare Formation contains multiple ~1–2‰ oscillations that generally trend more negative (to a nadir of ~–31‰ below and within the Aberdeen Member) and then shift to more positive values in the upper part of the formation. These Mount Hare strata host a number of positive shifts, including two in the Tremadocian Stage (TR1 and TR2) up to –28.1‰ and –29.1‰, respectively, and multiple poorly resolved excursions in the mid-Darriwilian and Katian that are only constrained by a few data points (Fig. 3). The Silurian portion of the Mount Hare and Tetlit formations is characterized by a series of prominent positive $\delta^{13}C_{org}$ excursions at ~1720 m, ~1770 m, ~1830 m, ~1910 m, and ~2000 m in the composite section, although some of these shifts are supported by a limited number of data points. $\delta^{13}C_{org}$ values also jump sharply around the J1609–J1610 section contact at ~2180 m in the Vittrekwa Formation (Fig. 3). Although the highest samples in J1609 trend positive, the majority of the shift occurs in the basal strata of section J1610 across a small fault between the sections. The overlying Vittrekwa strata are characterized by a broad negative trend from approximately –27.5 to –30.5‰, an increase to approximately –29.5‰ at ~2290 m, and then a negative trend to –31.4‰ near the top of the section. There is a sampling gap in the poorly exposed interval between 2414.1 and 2437 m, followed by relatively constant values averaging –30.5‰ at the top of the section.

Discussion

Paleoenvironmental interpretation

The Road River Group of the Richardson Mountains, Yukon, was deposited in a variety of basinal settings on the northwestern edge of the GACB. Facies associations 1–4, 6, and 7 most likely reflect a combination of hemipelagic suspension sedimentation, settling from dilute turbidity current tails or storm-generated plumes, and (or) bed-load deposition from waning low energy and (or) low volume grain- to mud-rich turbidity currents (Lowe 1982, 1988; Arnott and Hand 1989; Pilskaln et al. 1989; Wilber et al. 1990; Mulder and Alexander 2001). The rare very thin to thin coarse-grained interbeds indicate flows with abundant mud/silt- and relatively little sand-sized content (Mulder et al. 2014). The basal T_A divisions of these coarser-grained beds were most likely deposited during rapid suspension fallout from distal turbidity currents,

Table 5. Formalization of the Vittrekwa Formation, Road River Group.

Name	Vittrekwa Formation
Name derivation	Named after the Vittrekwa River within the northern Richardson Mountains, Yukon Territory, Canada; Eagle River and Trail River Quadrangles (NTS 116I and 106 L)
Category and rank	Lithostratigraphic Formation
Type area	Exposures along the Peel River, southwestern Richardson Mountains, Yukon Territory, Canada
Unit type section	Sections 15-TF-05–J1609–J1610 (Fig. 3; this paper) Located on south side of the Peel River ~1–4 km upstream of Aberdeen Canyon, Yukon Territory, Canada Lower boundary: gradational contact with upper Tetlit Formation (65.872833, 135.7577) Upper boundary: sharp contact with bedded chert of the Canol Formation (65.866016, 135.845633)
Historical nomenclature	Previously referred to as upper part of map unit CDr4 of Norris (1981*a*, 1981*b*, and 1981*c*), unit SDv of Cecile et al. (1982), and the "Vittrekwa Formation" of Morrow (1999)
Unit description	Variable succession of black shale, calcareous shale/siltstone, chert, and argillaceous limestone exposed throughout the Richardson Mountains. Basal contact with underlying strata of the Tetlit Formation is gradational and marked by an increase in calcareous shale content and decrease in coarser-grained lithofacies. Lower 92.9 m dominated by interbedded recessive dark grey to black calcareous and pyritic shale, calcisiltite, and fine-grained bioclastic to silicified grainstone with Bouma T_{ABCE} subdivisions, slump folds, synsedimentary truncation surfaces, convolute lamination, concretionary intervals, and localized bioturbation and crinoidal debris. The upper 10–20 m of these strata are duplicated in a small thrust fault at 93 m, which is then overlain by 100 m of dominantly dark grey to black calcareous and pyritic shale, silty lime mudstone, and calcisiltite with resistant intervals dominated by laminated or bioturbated calcisiltite. These strata locally contain concretionary intervals dominated by ~0.5–2 m wide calcareous concretions and local convolute lamination that dissipate up-section. This recessive interval is overlain by 110 m of more resistant and homogeneous calcisiltite, calcareous shale, and silty lime mudstone that contain tentaculids, local concretionary intervals, and zones of thin- to very-thin-bedded Bouma T_{BCE} subdivisions. These strata are overlain by 45 m of very poorly exposed calcareous shale, which are then overlain by 38 m of well-exposed interbedded silicified shale, calcareous mudstone, and siliceous calcisiltite to very-fine-grained grainstone that contain Bouma T_{CDE} subdivisions, local barite nodules and concretions, and abundant pyrite. These strata are abruptly overlain by the very-thin- to thin-bedded black to dark grey chert of the overlying Canol Formation.
Unit reference section	Reported but unmeasured ~72 m thick exposure along Trail River, Richardson Mountains (M. Cecile personal communication in Morrow 1999)
Dimensions	412.5 m thick at type section (Fig. 3, this paper); ~197 m thick in Caribou YT N-25 well
Geologic age	Silurian–Devonian (Pridoli(?)–Middle Devonian, or Givetian: Morrow 1999; this paper)
Regional correlations (shelf)	Peel, Tatsieta, Arnica, Landry, Hume, Ogilvie, Sombre, Delorme, Natla, Munch, McConnell, Stone, Nahanni, Dunedin, Ramhorn, and McDame formations of Alaska, USA, and Yukon, and Northwest Territories, Canada
Regional correlations (slope/basin)	McCann Hill Chert, Michelle, Mount Dewdney, Misfortune, Hailstone, Sapper, and Portrait Lake formations of Alaska, USA, and Yukon, and Northwest Territories, Canada

with transitions to T_B and T_C intervals indicating localized reworking (Arnott and Hand 1989). The majority of these fine-grained FAs are consistent with basin floor, lower slope, or distal levee or overbank sedimentation within the Richardson trough (Fig. 9A). The elevated TOC contents, spectacular graptolite preservation, and general lack of benthic fauna and trace fossils within these FAs suggest sedimentation under a dysoxic to anoxic water column well below storm wave base; however, there are discrete stratigraphic intervals dominated by heavy bioturbation, specifically within the upper Furongian, upper Darriwilian, lower–middle Katian, upper Aeronian, lower Telychian, and Lochkovian–Pragian (Fig. 3; Supplemental Material[1]). From a sedimentological perspective, these observations suggest that although deep basinal waters of the Richardson trough were generally anoxic, they were at least intermittently oxygenated enough to support infaunal activity at multiple points during its history.

Facies associations 5, 8, and 9 most likely reflect episodic high-energy sedimentation within the Road River Group. More specifically, FA 5 is dominated by normal graded to planar laminated dolosiltite and dolograinstone with occasional fossiliferous T_A lags, the combination of which reflect rapid suspension fallout from silt- and sand-rich, high-density turbidity currents (Lowe 1988; Arnott and Hand 1989; Mulder and Alexander 2001) in slope or basin-floor channel or levee complexes. The common association of this facies with slump deposits, soft-sediment deformation, and widespread bioturbation may reflect episodes of shoaling within the Richardson trough, perhaps into mid- to upper slope settings. In contrast, FAs 8 and 9 reflect slope or basin-floor deposition from carbonate-rich cohesive debris flows (e.g., Mulder and Alexander 2001) that were likely sourced from adjacent shallow-water carbonate platforms of the Yukon block and Mackenzie/Peel platform (Fig. 9A). The outsized clasts in these facies were likely supported by the cohesive strength of the mud-sized carbonate matrix (Mohrig et al. 1998; Mulder and Alexander 2001), and the associated slides most likely formed from failure and downslope movement of the upslope seabed (Arnott 2010). Episodic failure of the Richardson trough slope system is also supported by debris flow deposits that are solely composed of clasts from FAs 1–4 (Fig. 5H), a feature common to many steep-walled, intra-platform deep-water depocenters (Lynts et al. 1973; Harwood and Towers 1988; Grammer et al. 1993; Mulder et al. 2012). Finally, the presence of decametre-scale rafts of shelf and slope fragments in stacked megabreccia horizons (FA 9) of the Aberdeen Member (Mount Hare Formation) most likely reflects deposition from significant debris flows or mass transport complexes associated with a profound episode of base level fall and associated shelf-edge failure (e.g., Crevello and Schlager 1980; Mullins et al. 1991; Jo et al. 2015). This is supported by the presence of diverse allochthonous carbonate blocks in the megabreccia horizons that clearly experienced subaerial exposure and subsequent karstification prior to their transport into the trough. It is also possible that this facies reflects mass-transport sedimentation associated with syndepositional faulting in the Richardson trough, although there is no evidence for mid-Ordovician tectonism at this time.

A complex paragenetic history for Road River Group strata is supported by the occurrence of centimetre- to metre-scale carbonate, barite, and pyrite concretions (Figs. 3, 8E), all of which

Fig. 4. Selected photographs of the Cronin Formation and fauna, upper canyon of Peel River, Yukon. (A) View from helicopter looking northeast of section J1728 and the base of section T1701. Cliff height approximately 40 m. (B) Resistant outcrop style of Cronin Formation in section T1701. Geologist (circled) for scale. (C) Contact between Slats Creek and Cronin formations marked by appearance of fine-grained carbonate strata and loss of brown-weathering sandstone. Hammer (circled) for scale is 33 cm long. (D) Medium-bedded turbidites of FA 7 with distinct T_E recessive intervals at 192 m in T1701. Measuring stick is 10 cm long. (E) Erosional scour with subtle normal grading and secondary cubic pyrite in turbidites of section T1701. Mechanical pencil metal tip is 2.1 cm long. (F) Slump fold in section J1728 of the lower Cronin Formation. Hammer for scale is 33 cm long. (G–H) The agnostoid arthropod *Glyptagnostus reticulatus* from 217.5 m in section J1728; vertical white scale bar in each photo is 2 mm long: (G) cephalon and (H) pygidium. (I) Barite nodule (indicated by yellow arrow) in fine-grained strata of FA 4 from 235.4 m in section J1728. Hammer for scale is 33 cm long. [Colour online.]

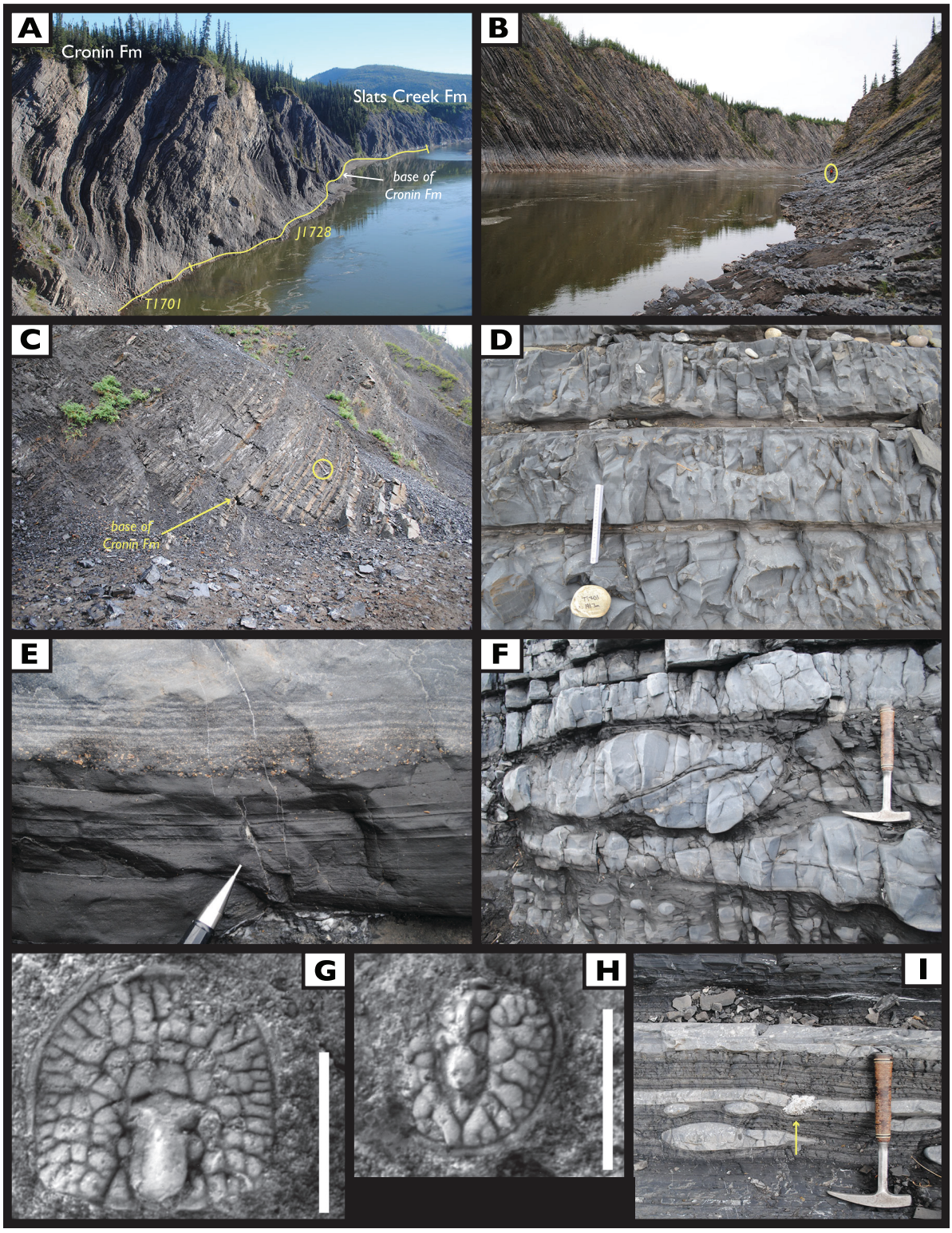

Fig. 5. Selected photographs of the Mount Hare Formation, upper canyon of Peel River, Yukon. (A) View looking west from helicopter of exposures with Aberdeen Canyon in background. Folded and displaced metre-thick debris flow marker-bed was traced to link up measured sections 17-TF-03 and J1727. (B) View looking east of Mount Hare Formation FA 4 just below Aberdeen Canyon. Geologist for scale. (C) View looking southeast of section J1611. Folds are clearly defined with white-weathering debris-flow deposit of FA 8; megabreccia sheet of basal Aberdeen Member defines the top of section J1611. (D) Ordovician–Silurian boundary interval in section J1518 above Aberdeen Canyon. Arrows mark the location of three marker debris-flow horizons of FA 8 with boundary interval highlighted by white dashed line. (E) Turbidite deposits and hemipelagic mudstone of FA 4 at ~70–85 m in section J1727 (~1340 m in composite section). Arrows above geologist's head mark slumped interval with chaotic bedding and slump folds. (F) Close-up of internal soft-sediment deformation within a T_D subdivision of FA 4. Pencil for scale is 14.2 cm long. (G) Close-up of Hirnantian paraconformity. Tip of hammer is pointing to bedding plane at 104.38 m in section J1518 or 1660.08 m in Fig. 3. The entire Hirnantian Stage is missing between this bedding plane and the first appearance of Rhuddanian (Llandovery) graptolites 14 cm above this level. (H) Exposed upper surface of slope-derived rudstone (FA 8) at 98 m in section J1518 (1653.7 m in composite section). Oxidized surface is from the weathering of a pyritic hardground. Hammer for scale is 33 cm long. [Colour online.]

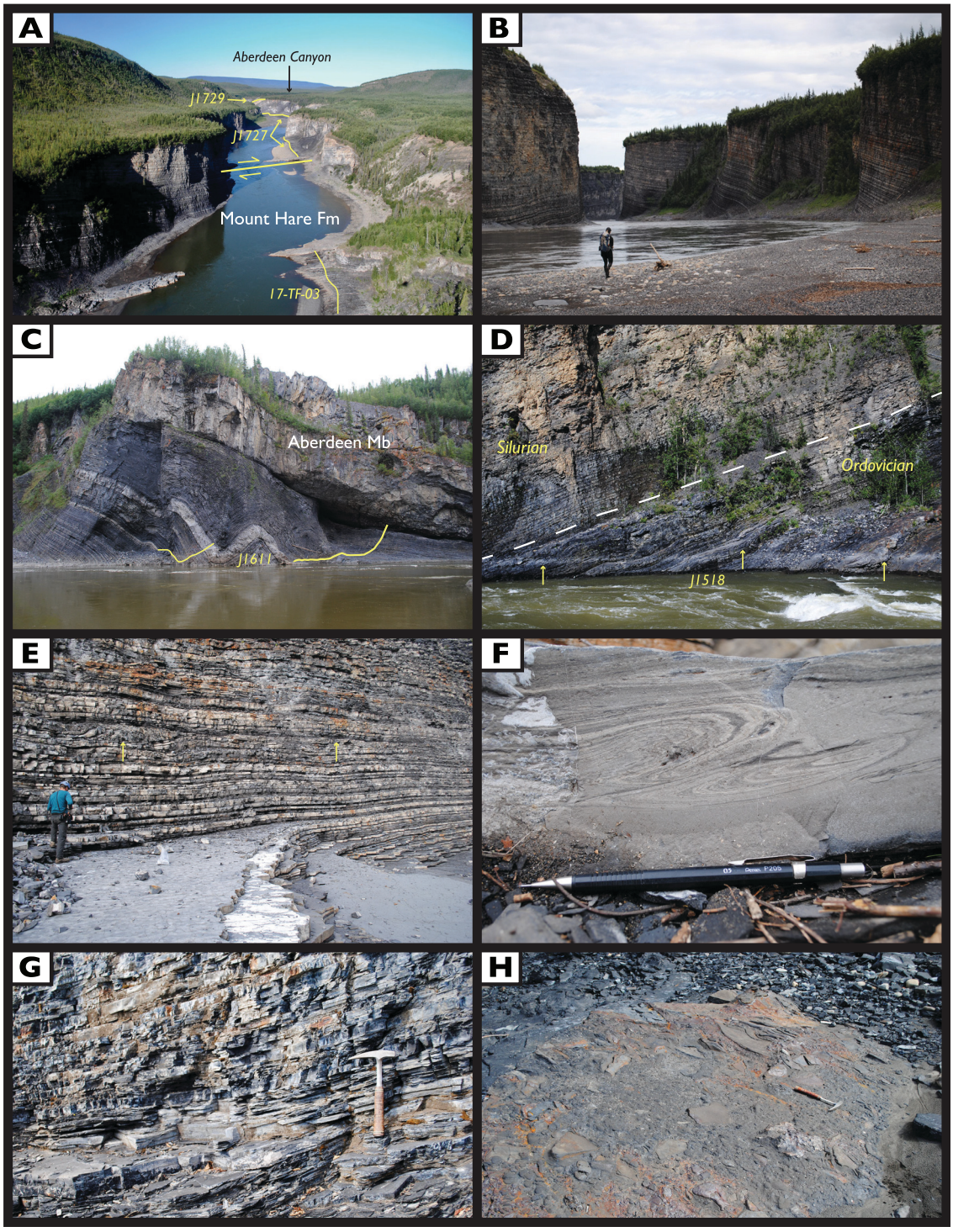

Fig. 6. Selected photographs of the Aberdeen Member of the Mount Hare Formation, Peel River, Yukon. (A) Photo from helicopter looking northwest of Aberdeen Canyon, which is formed by incision into thick-bedded strata of the Ordovician Aberdeen Member. (B) Geologist standing near basal surface of Aberdeen Member, which records an abrupt contact between fine-grained strata of FA 2 and 3 and massive thick-bedded rudstone, breccia, and megabreccia of FA 9. (C) Close-up of basal contact of Aberdeen breccia and rudstone with arrow pointing to internal deformation and small-scale duplication of underlying strata. Hammer (circled) for scale is 23 cm long. (D) Diverse shelf- and slope-derived clasts in rudstone and breccia near the base of the Aberdeen Member. Canadian penny (circled, 1.9 cm diameter) is resting on subangular light-grey microbial boundstone clast. (E) Dislocated raft of silicified black shale and mudstone within megabreccia of lower Aberdeen Member (23.5 m in section J1729 or 1552.3 m in composite section). Jacob staff for scale is 1.5 m tall. (F) Silicified karst breccia forming pod in subaerially-exposed raft of microbial boundstone and fossiliferous wackestone in uppermost megabreccia horizon of Aberdeen Member. Hammer for scale is 33 cm long. (G and H) show silicified breccia and boulders in uppermost debris sheet horizon of Aberdeen Member near the base of section J1518. Note how silicified black shale and mudstone drapes the uppermost horizon of the exhumed debris sheet. Hammer for scale is 33 cm long. [Colour online.]

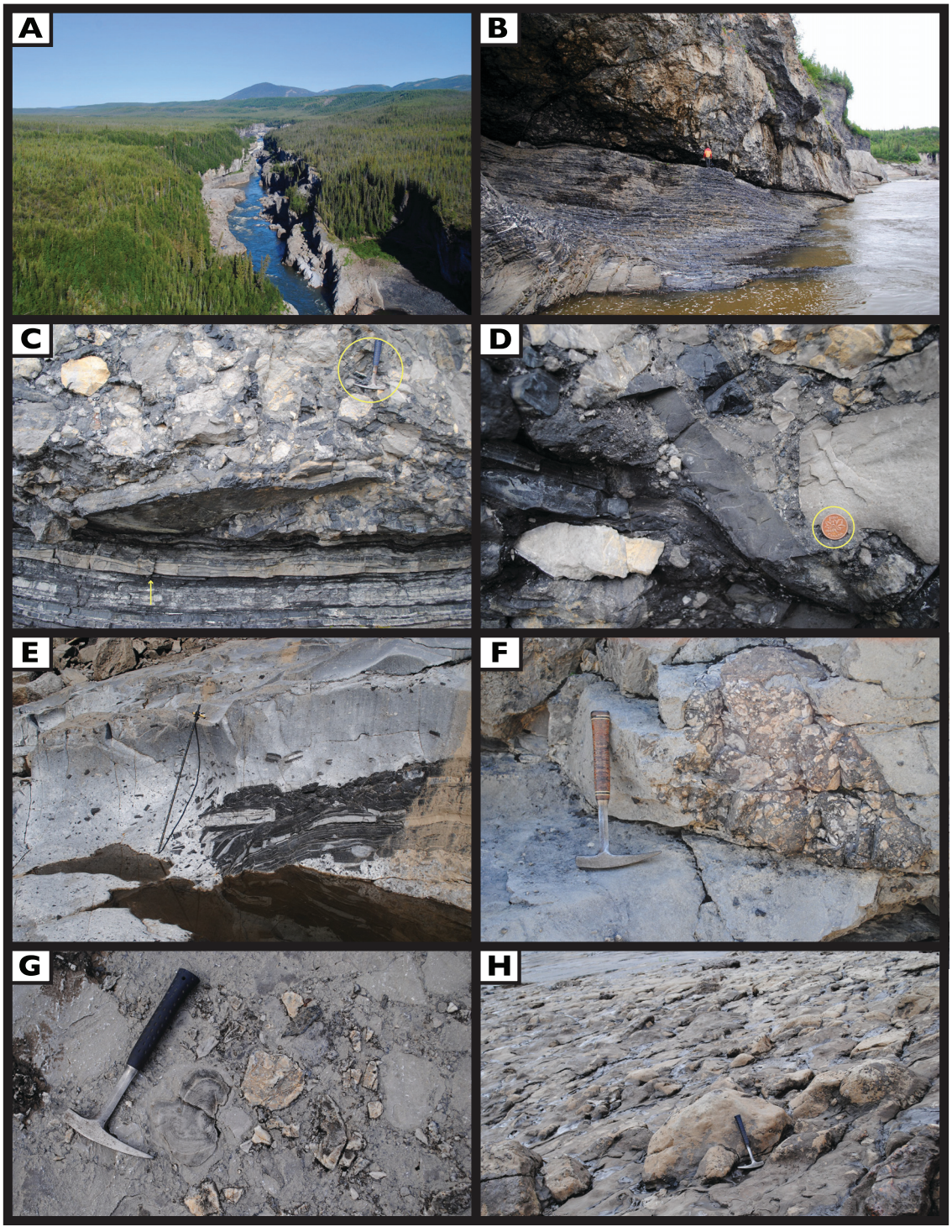

Fig. 7. Selected photographs of the Tetlit Formation, Peel River, Yukon. (A) View looking northwest across the Peel River at the contact between the Mount Hare and Tetlit formations. Note the distinct orange-weathering cliff-forming outcrops of medium- to thick-bedded dolosiltite and dolograinstone of FA 5. Cliff face is ~25 m tall. (B) Close-up view of the distinct weathering style of the Tetlit Formation at the base of section 15-TF-07; cliff face is ~25 m tall. (C) Metre-scale soft-sediment deformation below the circled hammer in the uppermost Mount Hare Formation directly beneath the first resistant beds of the Tetlit Formation. Hammer (circled) for scale is 33 cm long. (D) Prominent erosional scour of lithoclastic rudstone overlain by planar-laminated orange-weathering dolosiltite of FA 5. Coin (circled) for scale is 1.9 cm in diameter. (E) Soft-sediment deformation and small-scale faulting in white-weathering calcisiltite of FA 4 in the uppermost Tetlit Formation. Coin (circled) for scale is 1.9 cm in diameter. (F) Characteristic parallel-laminated orange-weathering dolosiltite and very fine-grained grainstone of the Tetlit Formation. Hammer for scale is 23 cm long. (G) *Chondrites* burrows in turbidites of the Tetlit Formation. Geologist's finger for scale. [Colour online.]

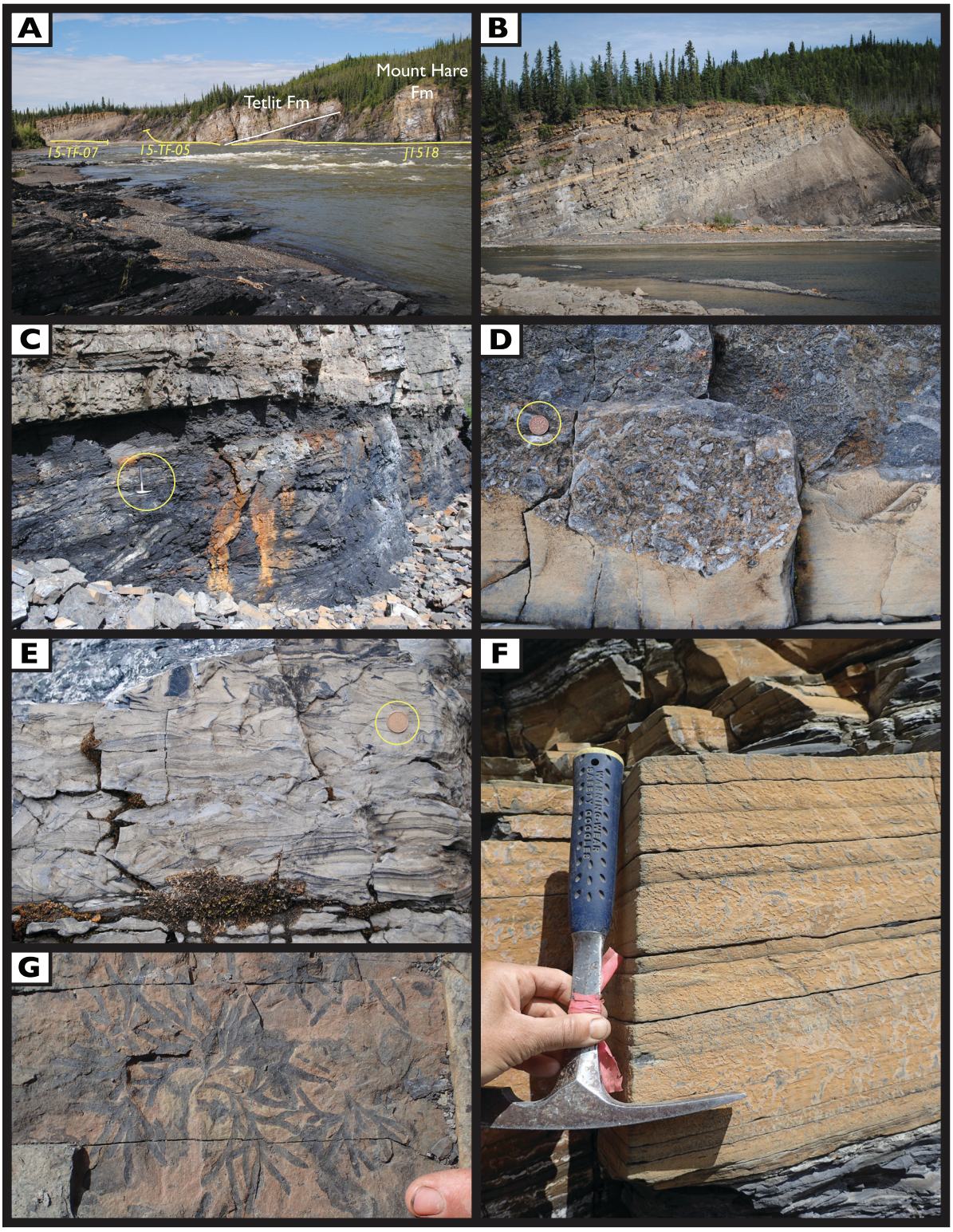

Fig. 8. Selected photographs of the Vittrekwa Formation, Peel River, Yukon. (A) Outcrop photograph of ~90–105 m interval in section J1610 (2272–2287 m interval in composite section of Fig. 3) highlighting the exposure of interbedded black shale and mudstone of FA 1. Geologist (circled) for scale. (B) Contact between the shale- and carbonate-dominated strata of the Vittrekwa Formation and orange-brown-weathering bedded chert of overlying Upper Devonian Canol Formation. The geologist's head is at a prominent carbonate and barite concretionary interval just directly below the Nick massive sulfide horizon, which weathers a prominent orange-white (arrows). (C) Syn-sedimentary truncation surface just above hammer handle in lime mudstone and calcisiltite of FA 2. Hammer for scale is 33 cm long. (D) Thin coarse-grained white-weathering interbed of fine-grained fossiliferous grainstone with soft-sediment deformation in FA 2. Coin for scale is 1.9 cm in diameter. (E) Metre-scale carbonate concretions nucleated around <10 cm thick coarse-grained interbeds in FA 1. Hammer (circled) for scale is 33 cm long. (F) Slump fold in lime mudstone and calcareous shale in section J1610. Coin for scale is 1.9 cm in diameter. (G) Silicified lime mudstone and calcareous shale just below the Vittrekwa–Canol contact in section J1610. Hammer for scale is 33 cm long. (H) Burrows with secondary pyrite concentrated on coarser-grained strata. Coin for scale is 1.9 cm in diameter. [Colour online.]

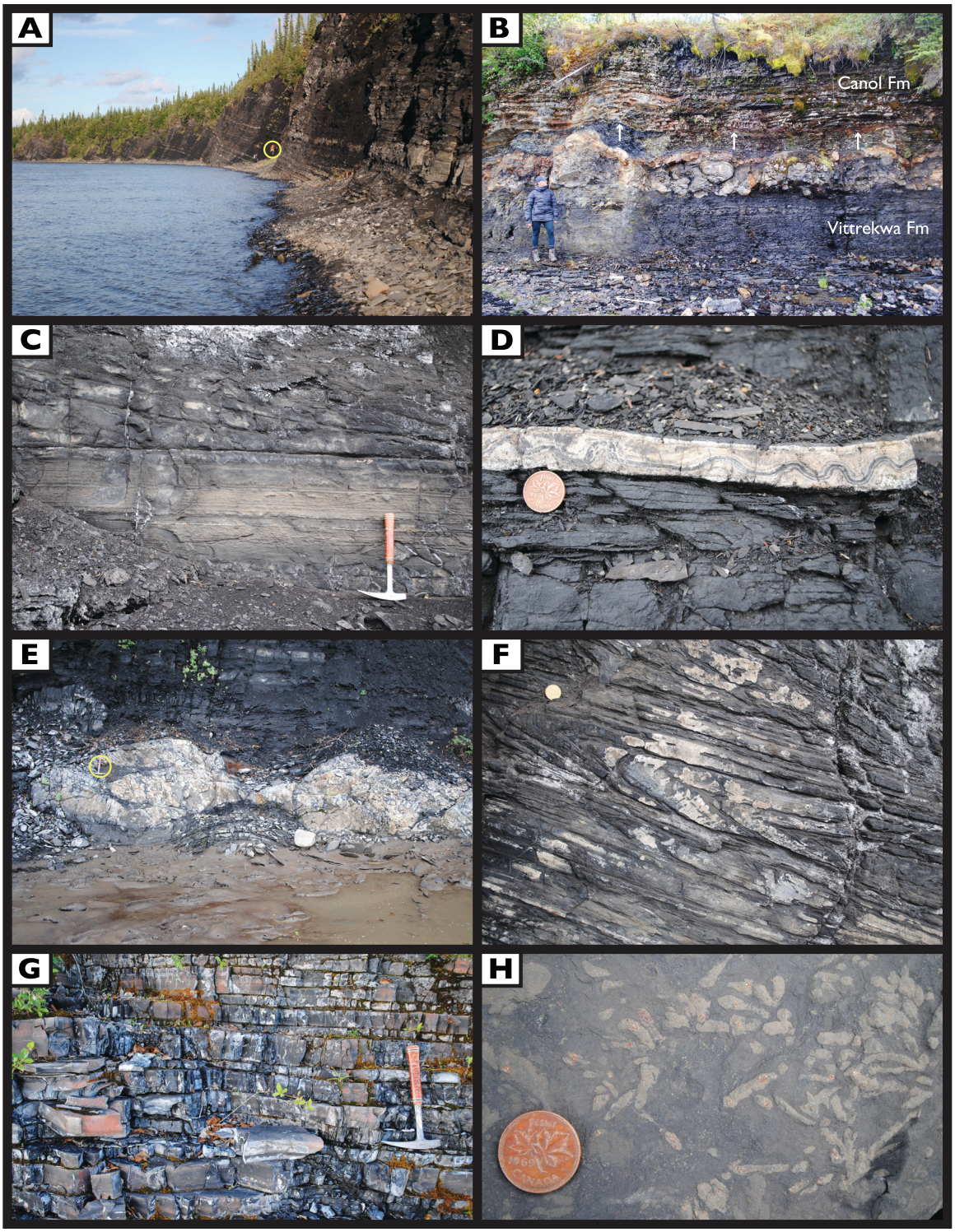

warrant future investigation through combined petrographic, microanalytical, and isotopic studies. For example, bedded chert and chert concretionary intervals in the Road River Group most likely reflect the replacement of primary carbonate or siliciclastic facies instead of representing deep-water silica sedimentation below the carbonate compensation depth (sensu Morrow 1999). This is broadly evidenced by siliceous concretionary textures forming selectively within coarser-grained beds, gradational contacts between chert horizons and other fine-grained lithofacies, and petrographic examinations of boundary zones adjacent to chert nodules and other stratiform chert horizons (Innis 1980). Rare volcanic detritus (Innis 1980) and very thin tephra horizons are also present within chert-dominated intervals of the Road River Group (Fig. 3); together with more ubiquitous biogenic sources of SiO_2, such as sponge spicules and radiolarian tests, these may have provided ample sources of remobilized $SiO_{2(aq)}$ during episodes of sedimentary condensation and (or) diagenesis.

Age of the Road River Group

Within the context of this long-lived intra-platformal basin, the combined biostratigraphic and chemostratigraphic data presented herein indicate that the Road River Group on the upper canyon of the Peel River preserves an almost complete record of early- to middle-Paleozoic deep-marine sedimentation (Lenz and Pedder 1972). There are exceptions, however; specifically, there are two identified unconformities in the section, and two intervals where time may be missing. Two of the possible missing intervals occur across discrete fault planes that cut the measured sections. Below, we explore these key missing time intervals and review portions of the stratigraphy that can be correlated globally to bolster our new age model for the Road River Group in the Richardson trough of Yukon.

The first missing time interval occurs at the Cronin/Mount Hare contact (T1701–17-TF-03 section boundary), where $\delta^{13}C_{carb}$ values abruptly shift more negative across a prominent dextral strike-slip fault (Figs. 2, 3; Supplementary Figs. S2, S3[1]). Although the most parsimonious interpretation is that there is missing section along this structure, the documented negative excursion in our composite section may still reflect the Cambrian–Ordovician boundary anomaly (Azmy et al. 2014; Edwards and Saltzman 2016; Scorrer et al. 2019; Wang et al. 2019). A comparison of the $\delta^{13}C_{carb}$ patterns seen in the lower 80 m of the 17-TF-03 section (Fig. 3; Supplementary Fig. S3[1]) with those documented in strata spanning the Cambrian–Ordovician boundary at Green Point, Newfoundland (the global stratotype of the base of the Ordovician; Azmy et al. 2014), as well as a correlative section in China (Wang et al. 2019) and elsewhere in Newfoundland (Scorrer et al. 2019), shows a very similar pattern with a negative excursion in the uppermost Cambrian, followed by a generally two-stepped increase in $\delta^{13}C_{carb}$ values (with some high-frequency fluctuations) before reaching a positive peak in the lowest Ordovician (Tremadocian). In the Newfoundland and Chinese sections, the biostratigraphically defined base of the Ordovician occurs after the first of the two steps in the rising values. In support of this, the lowest sample of the Tremadocian *Staurograptus dichotomous – Rhabdinopora parabola* Zone occurs at 64 m in the 17-TF-03 section (1160.2 m in the composite section of Fig. 3). Shortly above this level, there are a series of isotopic excursions that appear to accurately reproduce Tremadocian global $\delta^{13}C$ trends, including the TR1 and TR2 excursions, a long negative trend towards the Tremadocian–Floian boundary, and the Floian positive trend towards the Floian–Dapingian boundary (Bergstrom et al. 2009; Saltzman 2005; Saltzman and Thomas 2012; Edwards and Saltzman 2014; 2016; Edwards et al. 2018). For these reasons, we tentatively place the base of the Ordovician at ~1151.2 m in our composite section (Fig. 3; Supplementary Fig. S3[1]), while acknowledging that it is likely there is missing section beneath the fault plane in the terminal Cambrian (Stage 10, uppermost Furongian).

Another fault disrupts Lochkovian strata at the J1609 and J1610 section boundary (Fig. 3; Supplementary Figs. S8–S9[1]). The top of section J1609 contains the Early Devonian graptolite *Neomonograptus aequabilis*, indicative of the Lochkovian *Uncinatograptus uniformis* Zone, and $\delta^{13}C_{org}$ values trend positive, representing what we suggest may be the onset of the Klonk excursion at the Silurian–Devonian boundary (Husson et al. 2016 and references therein). The other side of the fault (at 6.95 m in section J1610) contains Pragian *Neocolonograptus falcarius* Zone graptolites. This is broadly consistent with, although slightly younger than, the age suggested by *Ogilviella* brachiopods in this interval, and indicates minimal Lochkovian strata in our section. The Silurian–Devonian boundary is complete in other areas of the Richardson trough (Lenz 1988), and more detailed biostratigraphic and focused stratigraphic examination of this interval along the upper canyon of the Peel River will likely provide enhanced resolution on how much time, if any, is missing locally along this structure.

In contrast with post-depositional faulting or lack of ample biostratigraphic data, two of the documented unconformities in our composite section represent subtle bedding-plane paraconformities. The first is between the uppermost Floian *Isograptus victoriae lunatus* Zone and the basal Darriwilian *Undulograptus austrodentatus* Zone (Fig. 3; Supplementary Fig. S5[1]). Based on our observations and collections, the entire Dapingian Stage is either missing or extremely condensed across a monotonous succession of silicified black shale and chert of FA 3 between 2.4 and 4.2 m in section J1611 of the Mount Hare Formation (Supplementary Fig. S5[1]; or 1507.3 and 1509.1 m in Fig. 3). In this respect, the upper canyon of the Peel River is quite different from the lower canyon of the Peel River (on the opposite side of the Deslauriers Fault, Fig. 1), where Dapingian strata containing *Parisograptus caduceus australis* Zone graptolites are locally present (Jackson and Lenz 2006; the reference to possible Dapingian samples in the upper canyon locality based on collections from Lenz and Pedder (1972) is likely incorrect—see Supplemental Material[1]).

The second bedding-plane paraconformity occurs between the uppermost Katian *Paraorthograptus pacificus* Zone (present at J1518–104.38 m in Supplementary Fig. S6[1] or 1660.08 m in Fig. 3) and the first Silurian strata 14 cm higher (combined *Akidograptus ascensus – Parakidograptus acuminatus* Zone). Here, the entire Hirnantian stage is either extremely condensed or missing in these 14 cm, with no physical evidence for erosion across a similar package of silicified shale and chert of FA 3 (Fig. 5G; see also Lenz and McCracken 1982). The underlying Katian interval of the Mount Hare Formation (Fig. 5D) is characterized by multiple debris-flow deposits of FA 8 capped by pyritized hardground surfaces (Fig. 5H) and interbedded with silicified shale and mudstone. These shelf- and slope-derived debris-flow horizons may reflect regional base-level fall associated with Katian–Hirnantian cooling. The Rock River locality ~75 km to the north in the Richardson Mountains is also unlikely to contain Hirnantian strata based on our preliminary investigations and the results of Lenz and McCracken (1982). Yet, to the south in the Blackstone trough (Fig. 1), LaPorte et al. (2009) reported >15 m of Hirnantian strata in the Road River Group, with biostratigraphic evidence for both Hirnantian graptolite zones (Loxton 2017) and a clear positive $\delta^{13}C_{carb}$–$\delta^{13}C_{org}$ excursion related to the Hirnantian isotopic event. This highlights that localized intervals of sedimentary bypass, submarine erosion, or extreme condensation in physically connected basinal settings should be considered in geochemical investigations of other deep-water sedimentary successions.

In spite of these known and possible minor gaps in the stratigraphic record of the Road River Group along the upper canyon of the Peel River, it is still a remarkably thick and largely continuous deep-marine record spanning ~110 million years of early to middle Paleozoic Earth history. To our knowledge there is no other outcrop section in the world with this level of near-continuous sedimentation, complete exposure, and limited structural deformation.

Table 6. Summary of Road River Group facies associations (FA), Richardson Mountains, Yukon, Canada.

Facies associations	Composition	Bedding style/structures	Depositional mechanism/environment	Distribution
FA 1: Shale or mudstone	Black- to dark-grey shale or mudstone; ~0.15–8.5 wt.% total organic carbon; partially to completely silicified locally; rare carbonate or chert nodules; locally disseminated to abundant calcite, dolomite, Fe-oxides, pyrite, sphalerite, and barite; gradational into FA 2 and locally interbedded with other FAs.	Typically structureless to planar-laminated, fissile, and recessive; commonly graptolitic and unbioturbated; form monotonous decametre-thick stratal units or interbeds in coarser-grained facies; very-thin to indeterminate bedding with sharp, planar basal contacts and rare undulatory upper contacts due to local erosion.	Hemipelagic suspension sedimentation or suspension settling from dilute turbidity current tail; silicification a combination of primary silica-rich contribution from sponge spicules and/or radiolarians or post-depositional diagenetic mobilization of silica; lower slope, basin-floor, and/or distal levee setting.	All formations
FA 2: Calcareous shale or mudstone	Black- to light-grey calcareous shale or mudstone; ~0.15–8.5 wt.% total organic carbon; rarely silicified; abundant calcite and dolomite nodules and concretions; disseminated to abundant pyrite and barite; some beds with <1 cm thick basal calcisiltite, wackestone, or grainstone; gradational into FA 1 and widely present in close association with other FAs.	Typically structureless to planar-laminated, resistant but locally recessive; bioturbation common; locally graptolitic forms monotonous decametre-thick stratal units or interbeds in coarser-grained facies; thin to indeterminate bedding with sharp, planar basal contacts and rare undulatory upper contacts; occasional slump folds, synsedimentary truncation surfaces, and chaotic internal lamination; grading common with thin interbeds.	Hemipelagic suspension sedimentation, suspension settling from dilute turbidity current tail, bed-load deposition from low-concentration, low-energy, fine-grained turbidity currents or storm-generated plumes; very thin basal coarse-grained interbeds indicate flows with abundant mud/silt content and low sand-sized content; calcareous material likely sourced from surrounding shallow carbonate platforms.	All formations
FA 3: Chert and silicified shale	Dark-grey to black bedded to replacive chert and silicified shale; composed of microcrystalline silica with disseminated crystals of calcite, dolomite, and pyrite; occasional hints of unidentified radiolarians or sponge spicules; gradational into or replacive of other fine-grained FAs.	Very-thin- to thick-bedded with occasional parallel to wavy lamination; commonly fabric destructive and associated with intervals of coarse-grained FAs, concretionary zones, or compaction-related chaotic bedding; tend to be fully replacive or nucleated on coarser-grained beds or lenses; locally graptolitic.	Presence of biogenic silica sources may indicate primary hemipelagic sedimentation in a basin-floor to slope setting; post-depositional fabrics suggest diagenetic mobilization and replacement of primary carbonate or siliciclastic FAs.	All formations
FA 4: Interbedded limestone, shale and mudstone	Light-grey to black lime mudstone, calcisiltite, wackestone, and very-fine- to very-coarse-grained grainstone interbedded with yellowish grey to black lime mudstone and shale; local lenticular to stratiform intervals of fossiliferous packstone; ferruginous to sulfidic shale drapes and black chert common with intervals displaying partial to complete silicification; locally pyritic with occasional pyrite concretions; gradational to abrupt transitions into all documented FAs; the most common FA in the Road River Group.	Thin- to medium-bedded with consistent display of partial to complete Bouma subdivisions; planar to undulatory bases and tops of beds; local lenticular geometries of coarser facies with distinct erosional bases; slump folds, synsedimentary truncation surfaces, and soft-sediment deformation present; variable proportions of limestone to shale/mudstone, but separated herein from FA 6 and FA 7 by >50% fine-grained strata; bed thickening and thinning trends are locally apparent, but remarkably consistent in instances; commonly graptolitic and locally bioturbated.	Ranges from hemipelagic suspension sedimentation to deposition from waning grain- to mud-rich turbidity currents; coarser-grained basal T_A division deposited during rapid suspension fallout from high-density turbidity currents with transitions to T_B and T_C indicating reworking of T_A by tail of turbidity current; T_{DE} sedimentation from dilute tail of flow or hemipelagic fallout; consistent with proximal to distal deep-marine levee or channel sedimentation with carbonate derived from platforms.	All formations

Table 6 (*continued*).

Facies associations	Composition	Bedding style/structures	Depositional mechanism/environment	Distribution
FA 5: Dolosiltite and dolograinstone	Buff yellow- to orange-weathering dolosiltite/calcisiltite and argillaceous dolograinstone; locally siliceous with abundant disseminated pyrite; some beds with basal ~1–10 cm dominated by fossiliferous grainstone or wackestone with local mudstone or shale intraclasts; some beds capped with planar or ripple cross-stratified dolograinstone or dolosiltite overlain by fine-grained strata of FA 1, FA 2, or FA 4.	Medium- to thick-bedded and resistant cliff-former; occasionally laminated to massive with sharp basal surfaces and planar to gradational upper surfaces displaying normal grading; bioturbation and chert nodules common to absent; commonly stratiform and regular; rare slump-folded intervals or chaotic lamination in fine-grained strata below or interbedded with dolosiltite/dolograinstone facies; Bouma subdivisions T_{ABC} with T_{DE} caps.	Rapid suspension fallout from silt- and sand-rich carbonate high-density turbidity currents in slope or basin-floor channel or levee complexes; source from storm-generated plumes also possible.	Only Tetlit Formation
FA 6: Parted to ribbon-bedded lime mudstone	Blueish-grey to dark-grey parted to ribbon-bedded lime mudstone, calcisiltite, and calcareous shale with rare <1 cm thick basal wackestone or very-fine-grained grainstone interbeds; local calcareous shale drapes commonly <5 cm thick; black chert nodules common; grainstone interbeds locally fossiliferous with articulate and inarticulate brachiopod debris; commonly gradational into FA 4 and FA 7.	Very-thin- to medium-bedded with planar to wavy bounding surfaces; mostly featureless with local planar lamination and ripple cross-lamination; rare slump folds and chaotic soft- sediment deformation; bioturbation common and locally abundant; rare dendroidal graptolite fauna; mostly >70% lime mudstone with thin calcareous shale partings; local preservation of Bouma T_{CDE} or T_{DE} subdivisions.	Hemipelagic suspension sedimentation, suspension settling from dilute turbidity current tail, bed-load deposition from low-concentration, low-energy, fine-grained turbidity currents or storm-generated plumes; very thin basal coarse-grained interbeds indicate flows with abundant mud/silt content and low sand-sized content; calcareous material likely sourced from surrounding shallow carbonate platforms.	Only Cronin and Vittrekwa formations
FA 7: Medium- to thick-bedded limestone	Blueish-grey to dark-grey interbedded lime mudstone, calcisiltite, wackestone, and grainstone with <5 cm thick black calcareous shale interbeds; grainstone interbeds locally fossiliferous with articulate and inarticulate brachiopod debris; black chert nodules locally present; commonly gradational into FA 4 and FA 6.	Medium- to thick-bedded with planar to irregular bounding surfaces with local evidence for erosion; planar-laminated, cross-laminated, or massive with local normal grading; bioturbation and dendroidal graptolite fauna rare; slump folds and soft-sediment deformation locally common with complete to partial Bouma subdivisions throughout.	Rapid suspension fallout from silt- and sand-rich carbonate high-density turbidity currents in slope or basin-floor channel or levee complexes; fine-grained intervals representative of hemipelagic rainout or deposition from dilute tail of turbidity flows; source from storm-generated plumes also possible.	Only Cronin Formation
FA 8: Shelf- and slope-derived rudstone and breccia	White to dark-grey clast- to matrix-supported intraclast rudstone and/or breccia; clasts range from pebble to boulder with derivation from allochthonous platform sources and FA 1 – FA 5; chert and secondary silicification common with abundant cubic and concretionary pyrite; shale intraclasts common.	Generally poorly sorted and stratiform in geometry with sharp basal contacts and little evidence for local erosion; sub-rounded to angular clasts either locally derived or from exotic shallow-water facies, including reef blocks, microbial and oolitic dolostone, silicified pisolites, and a wide variety of articulated and disarticulated fossil debris; internal shear surfaces rare, locally associated with slump folds, chaotic bedding, soft-sediment deformation, and concretions; locally normal graded into Bouma T_A, T_{BC}, or T_{CDE} divisions.	Deposited from carbonate-rich (cohesive) debris flows that were sourced from a shallow-marine carbonate platform; clasts supported by the cohesive strength of the mud-sized carbonate matrix.	Only Mount Hare, Tetlit, and Vittrekwa formations

Table 6 (*concluded*).

Facies associations	Composition	Bedding style/structures	Depositional mechanism/environment	Distribution
FA 9: Boulder rudstone/ Megabreccia	White to light grey clast- to matrix-supported rudstone and megabreccia with clasts ranging from pebble to slab with derivation from allochthonous platform sources and FA 1 – FA 5; shale intraclasts common; the main FA of the Aberdeen Member.	Poorly sorted, very-thick-bedded stratiform unit with irregular to sharp basal contact; strata beneath commonly deformed; sub-rounded to angular clasts or blocks either locally derived or from shallow-water facies, including coral reef debris, microbial and oolitic dolostone, karst breccia, and a variety of articulated and disarticulated fossil debris; internal shear surfaces rare, but locally associated with slump folds, chaotic bedding, and soft-sediment deformation; upper parts of flows normal graded into Bouma T_A, T_{BC}, or T_{CDE} divisions.	Deposited from carbonate-rich (cohesive) debris flows that were sourced from a shallow-marine carbonate platform; clasts supported by the cohesive strength of the mud-sized carbonate matrix; slides formed from failure and downslope movement of the upslope seabed; localized internal shear from movement along shear planes during mass movement.	Only Mount Hare Formation

Perhaps not surprisingly given the completeness of the section, our chemostratigraphic results identify multiple carbon isotopic events for the first time in the northern Canadian Cordillera. For example, the upper Cambrian Steptoean positive isotopic excursion (SPICE) event is clearly recorded in both $\delta^{13}C_{carb}$ and $\delta^{13}C_{org}$ measurements from the Cronin Formation (Fig. 3; Supplementary Fig. S1[1]) and is confirmed by the presence of *Glyptagnostus reticulatus* near the onset of the excursion (Saltzman et al. 2000; Peng et al. 2004; Gill et al. 2011). Notably, like other sections worldwide, the magnitude of the SPICE $\delta^{13}C_{carb}$ excursion is approximately two times greater than the $\delta^{13}C_{org}$ excursion (Saltzman et al. 2011). In addition, our new $\delta^{13}C_{carb}$ data from post-SPICE strata of the Cronin Formation constitutes one of the thickest and most expanded Furongian carbon isotope records to date (e.g., Saltzman et al. 2000, 2004; Saltzman and Thomas 2012; Li et al. 2017; Miller 2019; Wang et al. 2019). Unfortunately, however, the current lack of detailed biostratigraphic data from these strata makes it challenging to perform detailed correlations with other global sections (Li et al. 2017).

As highlighted previously, we have identified the Tremadocian TR1 and TR2 excursions, along with consistent Tremadocian–Floian negative and Floian positive trends (Edwards and Saltzman 2016; Edwards et al. 2018). Our current isotopic dataset does not permit confident recognition of many of the previously well-documented positive excursions through the Middle Ordovician to early Llandovery (Aeronian) interval (e.g., Saltzman and Thomas 2012); nevertheless, there do appear to be intervals of elevated $\delta^{13}C_{org}$ values, each marked by only one or a few samples, in the stratigraphic intervals in which we would expect to find the mid-Darriwilian event (Buggisch et al. 2003; Ainsaar et al. 2010), the lowest Katian Guttenberg excursion (Ludvigson et al. 2004; Young et al. 2005; Edwards and Saltzman 2016), and the lower Aeronian excursion (Melchin and Holmden 2006; Melchin et al. 2015) (Fig. 3, Supplementary Figs. S4–S6[1]). It is likely that future higher resolution coupled biostratigraphic and chemostratigraphic studies of the Road River Group will permit more confident identification of these events, as well as the recognition of additional isotopic events throughout this interval.

Large positive $\delta^{13}C_{org}$ excursions are evident in the post-Rhuddanian Mount Hare, Tetlit, and Vittrekwa formations (Fig. 3; Supplementary Figs. S6–S8[1]), including the late Aeronian (*sedgwickii*) excursion (~+1.5‰; Cramer et al. 2011; Frýda and Storch 2014; McAdams et al. 2019), the Telychian Valgu event in the *Monoclimacis griestoniensis* – *Monoclimacis crenulata* Zone (~+2‰; Melchin et al. 2012; Hammarlund et al. 2019), the Ireviken or early Sheinwoodian Carbon Isotope Excursion spanning the Llandovery–Wenlock boundary (~+3‰; Munnecke et al. 2003; Cramer and Saltzman 2005; McAdams et al. 2019), the Lau excursion in the Ludfordian (~+6‰; Cramer and Saltzman 2007; Kaljo et al. 2007; Frýda and Manda 2013), and the Lockhovian Klonk excursion (Saltzman 2002; Buggisch and Mann 2004; Husson et al. 2016). We did not identify a distinct *Oktavites spiralis* Zone positive excursion (Hammarlund et al. 2019), although the uppermost isotopic data in that Zone do trend more positive (Fig. 3; Supplementary Fig. S7[1]). In addition, an abbreviated Mulde (mid-Homerian) excursion (Cramer et al. 2006; Kaljo et al. 2007; Calner et al. 2012) may be present in the lower ~35 m of section 15-TF-05 (or ~1890–1925 m in the composite section) or in the covered interval between the top of section 15-TF-07 and base of section 15-TF-05. Although the characteristic two peaks of this event cannot be clearly seen in our isotopic record, the timing (spanning much of the upper Homerian) and magnitude of the positive $\delta^{13}C_{org}$ values are consistent with those seen in data from other regions (e.g., Cramer and Saltzman 2007; Jarochowska and Munnecke 2016). Finally, the long positive to negative isotopic trend in $\delta^{13}C_{org}$ data from section J1610 up to the stratigraphically highest graptolite collection matches well with other Pragian–Emsian isotopic datasets (e.g., Becker et al. 2012).

Fig. 9. (A) Diagrammatic reconstruction of possible paleoenvironmental settings for Road River Group strata in the Richardson trough (modified from Schlager and Chermak 1979). Key components include delivery of sediment from adjacent shallow-water settings of the Mackenzie/Peel platform and Yukon block, as well as deposition in both basinal and slope settings. Debris sheets are represented by coarser-grained deposits of FAs 8 and 9, and may have been sourced from talus aprons or platform flanks during base-level fall or synsedimentary faulting. This schematic reconstruction only provides a snapshot of the potential morphology and setting of the Richardson trough, which was a long-lived early Paleozoic feature of the northern Cordillera. (B) Schematic and highly simplified surface-area comparison of ancient and modern intraplatformal basins (oriented north), including potential analog basins represented by the Tongue of the Ocean (TOTO) and Exuma Sound of the Great Bahamas Bank. These schematic reconstructions do not reflect morphological changes over time, and the sawtooth patterns reflect boundaries with the open ocean.

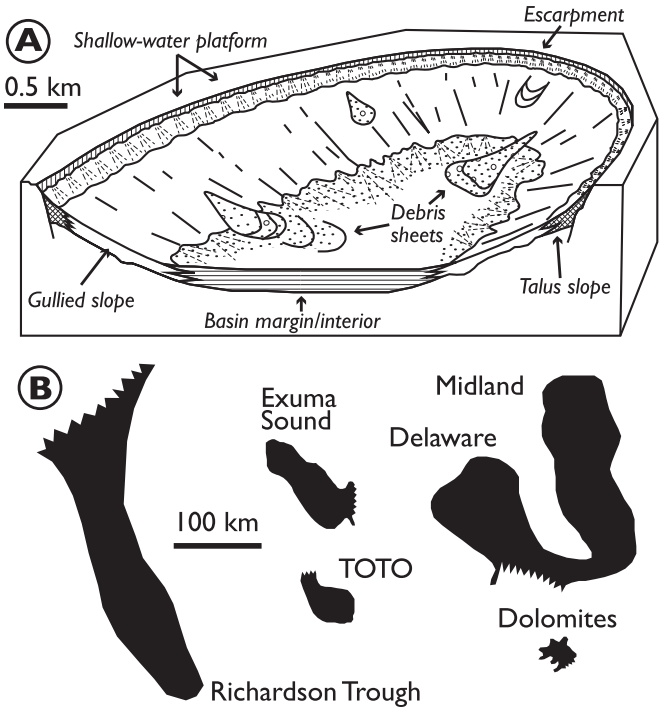

Depositional history of the Road River Group

We propose the Road River Group of the Richardson Mountains records similar depositional processes and environmental settings to other intra-platformal basins, such as portions of the Permian Midland and Delaware basins of Texas and New Mexico, the Cretaceous Tampico embayment of Mexico, and the modern Straits of Florida, Tongue of the Ocean (TOTO), or platformal terraces of the Great Bahamas Bank. Although the modern surface area of TOTO or Exuma Sound are much smaller than the Richardson trough (Fig. 9B), The widespread flanking by proximal shallow-water carbonate systems is a reasonable analog for the Richardson trough based on regional isopach patterns (e.g., Pugh 1983; Morrow 1999). In addition, the Road River Group records remarkably similar lithofacies to these modern analogs (e.g., Lynts et al. 1973; Schlager and Chermak 1979; Crevello and Schlager 1980; Grammer and Ginsburg 1992; Grammer et al. 1993), including abrupt interfingering of basin interior, slope, and debris sheet facies. Despite this, the lack of detailed regional sedimentological data from the Road River Group in the Richardson trough — besides what was previously reported by Jackson and Lenz (1962); Norford (1964); Innis (1980); Fritz (1997), and Morrow (1999) — precludes an attempt to extrapolate this depositional model beyond our study area to develop a more regional depositional system. In addition, all of these modern and ancient intraplatformal basins have evolved over time, so an individual snapshot of basin size or depositional system (e.g., Fig. 9B) is not necessarily representative of the entire setting. That being said, our observations at the upper canyon of the Peel River locality do suggest the Road River Group records deep-water sedimentation in the basin interior or lower–middle slope margins of the evolving Richardson trough (Fig. 9), which is consistent with previous observations (Lenz 1972; Innis 1980; Pugh 1983; Morrow 1999).

One of the most obvious features resulting from the revised age model of the Road River Group is the dramatically different rates of sediment accumulation between the Cronin Formation and the overlying Mount Hare, Tetlit, and Vittrekwa formations. Rough estimates suggest long-term formation accumulation rates of ~86 m/Myr for the Cronin Formation versus ~16 m/Myr, 12 m/Myr, and 8 m/Myr, respectively, for the other formations. We propose that this most likely reflects the regional subsidence history, with the pronounced late Cambrian sedimentation rates following early–middle Cambrian extension in northwestern Canada and the associated development of accommodation space in the nascent Richardson trough (e.g., Fritz 1997; Morrow 1999; Moynihan et al. 2019). Given that the Cronin Formation is both thick and has a consistent lithofacies composition (and, consequently, interpreted depositional setting), the elevated subsidence rates must have been compensated by ample carbonate production and sedimentation from the surrounding shallow-water platforms of the Yukon block and Mackenzie/Peel platform.

The contact of the Cronin Formation with underlying siliciclastic deposits of the Slats Creek Formation records a subtle deepening in the Richardson trough and widespread carbonate platform development in Yukon over the middle–late Cambrian (Fritz 1997; Morrow 1999; Pyle 2012). Slope gradients were low during Cronin sedimentation given the remarkably consistent facies assemblages across the Richardson Mountains (Lenz 1972; Innis 1980; Morrow 1999) and the lack of mass-flow deposits or submarine slumps (Fig. 3; Supplementary Figs. S1–S2[1]). This is also consistent with missing rimmed platform or shelf edge facies in the correlative shallow-water Jones Ridge, Bouvette, and Franklin Mountain formations and, therefore, may reflect sedimentation on a distally steepened carbonate ramp (Read 1982, 1985; Morrow 1999). Similar depositional models have been proposed for the age-equivalent Rabbitkettle Formation of the Mackenzie/Peel platform, Misty Creek embayment, and Selwyn basin (Gabrielse et al. 1973; Ludvigsen 1975, 1982; Cecile 1978; Cecile et al. 1982; Pratt 1988, 1992; Gordey and Anderson 1993; Fritz 1997), which has been correlated with the Cronin Formation in Yukon (e.g., Morrow 1999). In contrast, the Mount Hare, Tetlit, and Vittrekwa formations are characterized by basin-floor to slope sedimentary processes, including large-scale shelf and slope failure deposits, highlighting the regional development of more pronounced shelf-slope breaks with age-equivalent Ordovician–Devonian shallow-water deposits of the flanking Yukon block and Mackenzie/Peel platform. Unfortunately, the transitional facies between these regions are not well preserved and (or) lack detailed investigation in the Richardson trough, except at its southern termination near Royal Creek where the focus has mostly been on paleontological research (Lenz 1968, 1982; Fritz 1997; Norford 1997; Morrow 1999).

Morrow (1999) suggested that there was no evidence for lowstand sedimentation in the Road River Group associated with a regionally significant Middle Ordovician unconformity in the Mackenzie/Peel platform (the "sub-Mount Kindle unconformity"), which is equivalent in stratigraphic position to the Sauk–Tippecanoe megasequence boundary throughout Laurentia (e.g., Taylor et al. 2012 and references therein). Here, we suggest the Darriwilian Aberdeen Member of the Mount Hare Formation is a direct

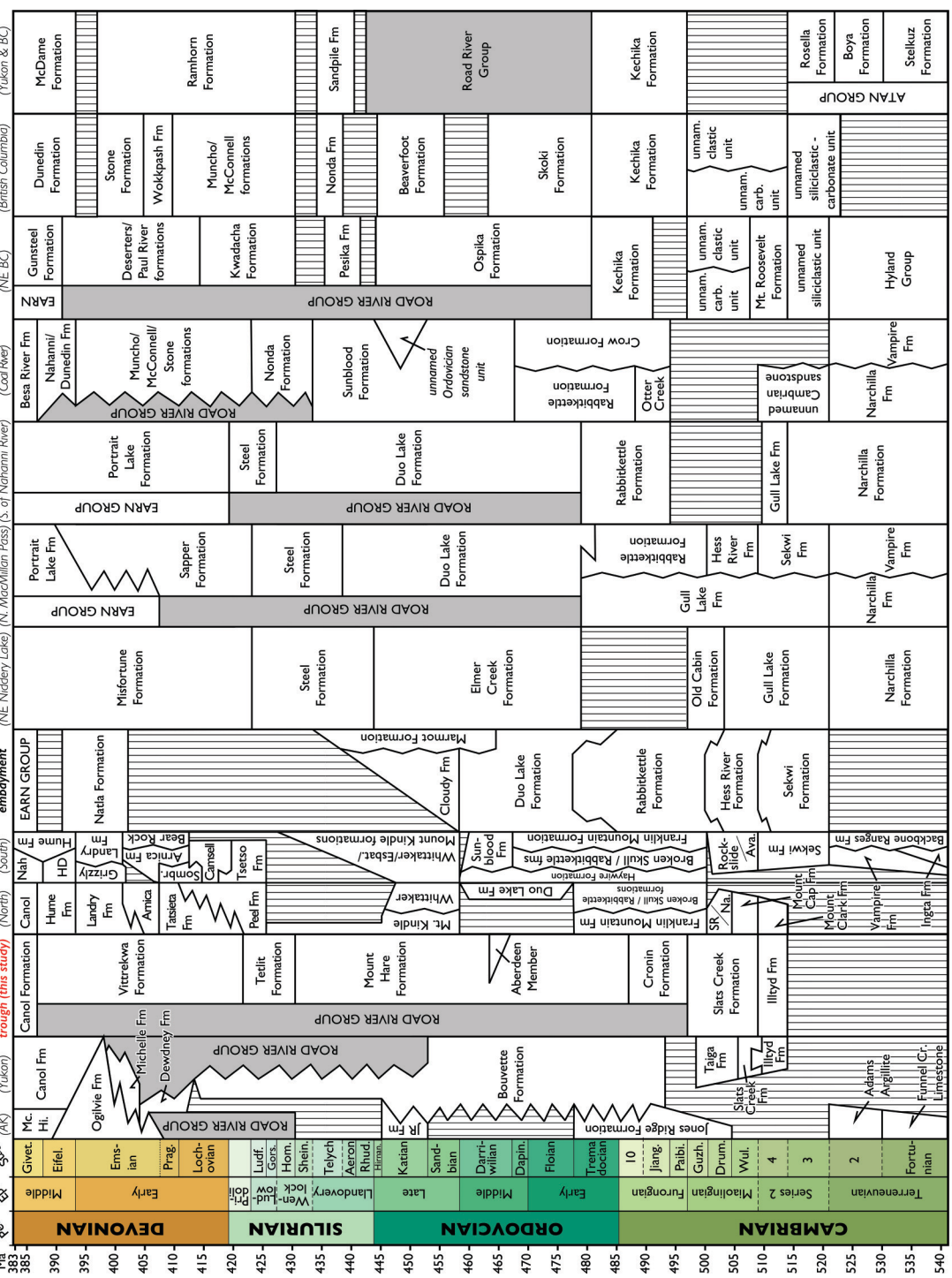

Fig. 10. Stratigraphic correlation diagram adapted from Morrow (1999) and Pyle (2012) of key platformal and basinal sedimentary successions in the northern Canadian Cordillera. References to individual localities are provided beneath each column with some comparisons discussed in the text. Data from Jackson and Lenz (1962), Brabb (1967), Gabrielse et al. (1973), Cecile et al. (1982), Pugh (1983), Gabrielse (1998), Fritz et al. (1991), Gordey and Anderson (1993), Fritz (1997), Ferri et al. (1999), Morrow (1999), Cecile (2000), Pyle and Barnes (2000, 2001, 2003), Pyle et al. (2003), Post and Long (2008), Gordey and Roots (2011), Abbott (2013), MacNaughton and Fallas (2014), MacNaughton et al. (2013, 2016), Pigage et al. (2015), and Taylor et al. (2015). See abbreviations listed in Fig. 3 for the geological timescale. Ava., Avalanche Formation; BC, British Columbia; Esbat., Esbataottine Formation; Fm, Formation; fms, formations; HD, Headless Formation; JR Fm, Jones Ridge Formation; Mc. Hi., McCann Hill Chert; Na., Nainlin Formation; Nah, Nahanni Formation; Sombr., Sombre Formation; SR, Saline River Formation; unnam., unnamed. [Colour online.]

sedimentary expression of this event, which is locally indicated by non-deposition at the Floian–Dapingian boundary, followed by the delivery of allochthonous shelfal material into the interior of the Richardson trough (Figs. 3, 6). A similar relationship is also developed during presumed Katian–Hirnantian base level fall, where uppermost Katian strata at the upper canyon of the Peel River locality host multiple debris flow deposits consisting of allochthonous shelf-derived material (Fig. 5D), which are followed by an interval of non-deposition across the entire Hirnantian Stage. Both of these paraconformities may be directly related to these global lowstands, either through short-lived condensation or non-deposition as a function of sedimentary bypass in this part of the Richardson trough, although their patterns of debris flow sedimentation and condensation are reversed in stratigraphic order.

In contrast with these Ordovician events, the lower Tetlit Formation records broader shoaling in the Richardson trough, consistent with regionally significant Silurian unconformities that are seen throughout platformal carbonates of Yukon, Alaska, and Northwest Territories (Morrow 1999). These events may be stratigraphically equivalent to the Tippecanoe–Kaskaskia megasequence boundary (Sloss 1963), which commonly consists of multiple amalgamated unconformities associated with Silurian glacio-eustatic lowstands. The upper Tetlit and Vittrekwa formations record the return to more distal slope depositional conditions, with sedimentation rates in the basin slowing to the lowest levels in the entire Road River Group by the end of Vittrekwa time (Gadd et al. 2020). Finally, the uppermost strata in the Road River Group record an episode of pronounced basinal condensation at the contact with the Canol Formation (equivalent to lowermost Earn Group strata in Selwyn basin (Fraser and Hutchison 2017)).

Regional stratigraphic correlations within the Northern Cordillera

The Road River Group has been at the heart of complex regional correlation schemes in the northern Canadian Cordillera for decades (Cecile 1978, 1982, 2000; Fritz 1985; Gordey and Anderson 1993; Morrow 1999; Pyle 2012). Much of the debate was originally centered around the use of "Formation" versus "Group" for these diverse deep-water strata, with subsequent controversy extending to stratigraphic ranges and widespread misuse in describing early to middle Paleozoic fine-grained successions throughout Alaska, Yukon, Northwest Territories, and northern British Columbia. Here, we mostly follow the original suggestion of Fritz (1985) in elevating the Road River unit to "Group" status and Cecile et al. (1982) and Morrow (1999) for more specific definitions of the base and top of the succession in the type area of the Richardson Mountains. Our main departure from Fritz (1985) is to redefine the base of the Road River Group in the Richardson trough to the first appearance of carbonate strata (Cronin Formation). Under this revised definition, the unnamed middle–upper(?) Cambrian shale unit of the Richardson Mountains (map unit CDr0 of Norris 1981*a*, 1981*b*, 1981*c*, 1982*a*, 1982*b*; Cecile et al. 1982) between the Cronin and Slats Creek/Illtyd formations should either be included with the Slats Creek Formation (Fig. 3) or separated as a new unit in future work. In addition, we differ from Cecile (1982) and Morrow (1999) in that we define a new upper Cambrian unit, the Cronin Formation, instead of propagating the "Rabbitkettle Formation" terminology of the Selwyn basin and Misty Creek embayment into the Richardson trough (Fig. 10). This decision is motivated by our poor understanding of the interconnectedness of these deep-water depocenters throughout the early Paleozoic (Lenz 1972; Pugh 1983; Fritz 1985).

Here, we propose that the term Road River Group should be restricted to basinal carbonate and siliciclastic strata that postdate the widespread upper Cambrian sub-Jiangshanian unconformity in Alaska, Yukon, Northwest Territories, and British Columbia. This not only provides a useful chronostratigraphic placement, but also separates this unit from the complex early–middle Cambrian facies changes associated with regional extension (Moynihan et al. 2019). Although this definition is already consistent with most established correlation schemes (Fig. 10), it implies some changes should be taken into consideration throughout the various paleogeographic elements of the northern Cordillera. For example, in the Misty Creek embayment and northern Selwyn basin regions (Fig. 1), we suggest the Hess River Formation should be separated from the Road River Group (Cecile 1982). Using our restrictive definition, one could propose that both the Rabbitkettle and Kechika (Gabrielse 1963) formations of Yukon, Northwest Territories, and British Columbia should be included in the revised Road River Group stratigraphic concept; however, we recommend restricting the usage of the Road River Group nomenclature as much as possible in future investigations. As a result, we highlight three options regarding Road River Group terminology in the northern Cordillera: (1) retain Road River Group within the various paleogeographic elements of the northern Cordillera but restrict its usage to reflect deep-water strata spanning from the sub-Jiangshanian unconformity to the base of the Devonian–Carboniferous Earn Group; (2) restrict the Road River Group to the Richardson trough type area and define new Group-level units in the Selwyn basin, Yukon block, Mackenzie/Peel platform, Kechika trough, and Cassiar terrane; or (3) retain the Road River Group nomenclature only in the Richardson trough and Selwyn basin and define new Group- and Formation-level units in the Yukon block, Kechika trough, Mackenzie/Peel platform, and Cassiar terrane. Our preference is option 1, as it has clear regional chrono- and tectono-stratigraphic significance. Future investigators should consider these choices when making new stratigraphic calls on deep-water Cambrian–Devonian strata throughout the northern Cordillera.

Conclusions

The Road River Group of the Richardson Mountains, Yukon, Canada, records basin interior to slope sedimentation in an intraplatform depocenter at the northwesternmost edge of the GACB. New data from the upper canyon of the Peel River, including sedimentological observations, stratigraphic and facies subdivisions, paleontological collections, and carbonate and organic carbon isotope chemostratigraphy enable the following significant conclusions:

(1) The newly defined upper Cambrian (Paibian–Furongian) Cronin Formation overlies the middle Cambrian Slats Creek Formation and consists of fine-grained carbonate and siliciclastic strata deposited in the interior of the Richardson trough or on the seaward edge of a late Cambrian carbonate ramp system that originated along the Yukon block or Mackenzie/Peel platform. New $\delta^{13}C_{carb}$ and $\delta^{13}C_{org}$ isotopic data from the Cronin Formation suggest it records the global SPICE event.

(2) The overlying newly formalized Mount Hare Formation of the Road River Group records diverse Lower Ordovician (Tremadocian)–Silurian (Wenlock) deep-water lithofacies that reflect basin interior to lower slope depositional environments. These strata host the newly defined Middle Ordovician (Darriwilian) Aberdeen Member, which records a discrete episode of debris-flow and (or) mass-transport sedimentation associated with regional base level fall at the Sauk–Tippecanoe megasequence boundary. Carbon isotope chemostratigraphic data from the Mount Hare Formation record the Tremadocian TR1 and TR2 events, the Katian Guttenberg excursion event, and multiple Llandovery positive $\delta^{13}C_{org}$ excursions (e.g., early and late Aeronian, Valgu, and Ireviken).

(3) The newly defined Silurian (Wenlock–Ludlow) Tetlit Formation of the Road River Group records a sharp transition to coarser-grained carbonate and siliciclastic slope deposits that may reflect broad shoaling within the Richardson trough or progradation of a deep-water channel and levee system over

the Peel River study area. These strata are distinguished by their decametre-scale alternation between yellow-weathering dolomitic dolosiltite/dolograinstone and recessive mudstone strata. New $\delta^{13}C_{org}$ data from the Tetlit Formation most likely record the Homerian Mulde and Ludfordian Lau positive carbon isotope excursions.

(4) The overlying newly formalized Silurian (Pridoli)–Middle Devonian (Givetian) Vittrekwa Formation of the Road River Group records a return to deep-water carbonate-dominated basin interior to slope sedimentation within the Richardson trough. New $\delta^{13}C_{org}$ data from the Vittrekwa Formation record the Lochkovian Klonk positive excursion, as well as a distinct Pragian–Emsian positive to negative carbon isotopic trend.

(5) Regional stratigraphic correlations of the Road River Group (Tables 2–5, Fig. 10) suggest the widespread development of deep-water depocenters within and along the edge of the GACB of Alaska, Yukon, and Northwest Territories. Our paleoenvironmental and paleogeographic reconstructions suggest this part of Laurentia was similar to the modern Great Bahamas Bank, with the Road River Group recording analogous deep-water sedimentation within intra-platformal basins, such as the TOTO or Exhuma Sound, or along the fringes of the bank system such as the Straits of Florida.

Acknowledgements

We are grateful to the Na Cho Nyak Dun and Tetlit Gwitch'in communities for granting us permission to work on the Peel River locality. This article is dedicated to Charlie Roots (1956–2016) of the Geological Survey of Canada who consistently encouraged J.V.S. to work on the Road River Group. Our field project was generously supported by the Yukon Geological Survey (YGS). In addition, J.V.S. was partially supported by Dartmouth College, the National Science Foundation (NSF) Tectonics Program (EAR–1624131), and an Agouron Institute Geobiology Postdoctoral Fellowship. J.M. was funded through the Undergraduate Research program (UGAR) at Dartmouth College. Geospatial support for this project was provided to J.V.S. by the Polar Geospatial Center under National Science Foundation-Office of Polar Programs (NSF-OPP) awards 1043681 and 1559691. E.A.S. was funded by NSF Division of Earth Sciences (EAR)-1922966 and the affiliates of the Stanford Project on Deep-water Depositional Systems. M.J.M. was funded by a Natural Sciences and Engineering Research Council of Canada (NSERC) Discovery Grant. We thank Tom Boag, Leigh van Drecht, Andrew Flower, Tom Laakso, Peter Mamrol, Richard Stockey, and Ginny Wala for field assistance; James Busch, Jennifer Howley, Karol Faehnrich, Peter Kannam, Charlotte Nutt, Max Saylor, Jack Taylor, Safia Khouja, Andrew Flower, Tessa Browne, Austin Miller, and Rachel Reid for help processing and analyzing samples in the laboratory; Una Farrell for help with data management; and Michael Orchard and Godfrey Nowlan for help identifying conodont specimens. Fireweed Helicopters provided safe and reliable transportation into the Richardson Mountains. Alf Lenz, Maurice Colpron, David Moynihan, and John Innis are thanked for providing stimulating and helpful conversations. Associate Editor George Dix, Brian Pratt, and an anonymous reviewer are thanked for their insightful and constructive feedback. This manuscript is YGS contribution No. 046.

References

Abbott, J.G. 1997. Geology of the upper Hart River area, eastern Ogilvie Mountains, Yukon Territory (116A/10, 116A/11). Indian and Northern Affairs Canada, Exploration and Geological Services Division, Yukon Region, 9. 92pp.

Abbott, J.G. 2013. Bedrock geology of the Macmillan Pass area, Yukon and adjacent Northwest Territories (NTS 105O/1, 2 and parts of 105P/4, 5) (1:50,000 scale). Yukon Geological Survey Geoscience Map 2013-1.

Ainsaar, L., Kaljo, D., Martma, T., Meidla, T., Männik, P., Nõlvak, J., and Tinn, O. 2010. Middle and Upper Ordovician carbon isotope chemostratigraphy in Baltoscandia: a correlation standard and clues to environmental history. Palaeogeography, Palaeoclimatology, Palaeoecology, **294**: 189–201. doi:10.1016/j.palaeo.2010.01.003.

Alroy, J., Aberhan, M., Bottjer, D.J., Foote, M., Fursich, F.T., Harries, P.J., et al. 2008. Phanerozoic trends in the global diversity of marine invertebrates. Science, **321**: 97–100. doi:10.1126/science.1156963. PMID:18599780.

Arnott, R.W.C. 2010. Deep-marine sediments and sedimentary systems. Facies Models, **4**: 295–322.

Arnott, R.W.C., and Hand, B.M. 1989. Bedforms, primary structures and grain fabric in the presence of suspended sediment rain. Journal of Sedimentary Research, **59**: 1062–1069. doi:10.1306/212F90F2-2B24-11D7-8648000102C1865D.

Azmy, K., Stouge, S., Brand, U., Bagnoli, G., and Ripperdan, R. 2014. High-resolution chemostratigraphy of the Cambrian–Ordovician GSSP: enhanced global correlation tool. Palaeogeography, Palaeoclimatology, Palaeoecology, **409**: 135–144. doi:10.1016/j.palaeo.2014.05.010.

Bambach, R.K., Knoll, A.H., and Sepkoski, J.J., Jr. 2002. Anatomical and ecological constraints on Phanerozoic animal diversity in the marine realm. Proceedings of the National Academy of Sciences, USA, **99**: 6854–6859. doi:10.1073/pnas.092150999. PMID:12011444.

Becker, R.T., Gradstein, F.M., and Hammer, O. 2012. The Devonian Period. *In* The geologic time scale 2012, Vol. 2. *Edited by* F.M. Gradstein, J.G. Ogg, M. Schmitz, and G. Ogg. Elsevier BV, Amsterdam, the Netherlands. pp. 559–601.

Beranek, L.P. 2017. A magma-poor rift model for the Cordilleran margin of western North America. Geology, **45**: 1115–1118. doi:10.1130/G39265.1.

Bergstrom, S.M., Chen, X., Gutiérrez-Marco, J.C., and Dronov, A. 2009. The new chronostratigraphic classification of the Ordovician System and its relations to major regional series and stages and to $\delta^{13}C$ chemostratigraphy. Lethaia, **42**(1): 97–107.

Blodgett, R.B., Potter, A.W., and Clough, J.G. 1984. Upper Ordovician-Lower Devonian biostratigraphy and paleoecology of the Jones Ridge-Squaw Mountain area, east-central Alaska. *In* Geological Society of America Abstracts with Programs. 270pp.

Bouma, A.H. 1962. Sedimentology of some Flysch Deposits. Elsevier, Amsterdam, the Netherlands. 168pp.

Brabb, E.E. 1967. Stratigraphy of the Cambrian and Ordovician rocks of east-central Alaska. U.S. Geological Survey, Professional Paper 559-A. 30pp.

Buggisch, W., and Mann, U. 2004. Carbon isotope stratigraphy of Lochkovian to Eifelian limestones from the Devonian of central and southern Europe. International Journal of Earth Sciences, **93**: 521–541. doi:10.1007/s00531-004-0407-6.

Buggisch, W., Keller, M., and Lehnert, O. 2003. Carbon isotope record of Late Cambrian to Early Ordovician carbonates of the Argentine Precordillera. Palaeogeography, Palaeoclimatology, Palaeoecology, **195**: 357–373. doi:10.1016/S0031-0182(03)00365-1.

Calner, M., Lehnert, O., and Jeppsson, L. 2012. New chemostratigraphic data through the Mulde Event interval (Silurian, Wenlock), Gotland, Sweden. GFF, **134**: 65–67. doi:10.1080/11035897.2012.670015.

Campbell, R.W., Beranek, L.P., Piercey, S.J., and Friedman, R. 2019. Early Paleozoic post-breakup magmatism along the Cordilleran margin of western North America: new zircon U-Pb age and whole-rock Nd- and Hf-isotope and lithogeochemical results from the Kechika Group, Yukon, Canada. Geosphere, **15**: 1262–1290. doi:10.1130/GES02044.1.

Canfield, D.E., and Farquhar, J. 2009. Animal evolution, bioturbation, and the sulfate concentration of the oceans. Proceedings of the National Academy of Sciences, USA, **106**: 8123–8127. doi:10.1073/pnas.0902037106.

Cecile, M.P. 1978. Report on Road River stratigraphy and the Misty Creek Embayment, Bonnet Plume (106B), and surrounding map areas, Northwest Territories. Current Research, Part A, Geological Survey of Canada, **78**(1): 371–377. doi:10.4095/103916.

Cecile, M.P. 1982. The Lower Paleozoic Misty Creek Embayment, Selwyn Basin, Yukon and Northwest Territories. *In* Geological Survey of Canada Bulletin, 335. 78pp.

Cecile, M.P. 2000. Geology of the northeastern Niddery Lake map area, east-central Yukon and adjacent Northwest Territories. *In* Geological Survey of Canada Bulletin, 553. 129pp.

Cecile, M., Hutcheon, I.E., and Gardner, D. 1982. Geology of the northern Richardson Anticlinorium. Geological Survey of Canada, Open File 875.

Cecile, M.P., Morrow, D.W., and Williams, G.K. 1997. Early Paleozoic (Cambrian to Early Devonian) Tectonic Framework, Canadian Cordillera. Bulletin of Canadian Petroleum Geology, **45**: 54–74. doi:10.35767/gscpgbull.45.1.054.

Churkin, M., Jr., and Brabb, E.E. 1965. Ordovician, Silurian, and Devonian biostratigraphy of east-central Alaska. American Association of Petroleum Geologists Bulletin, **49**(2): 172–185. doi:10.1306/A6633526-16C0-11D7-8645000102C1865D.

Colpron, M., Israel, S., Murphy, D., Pigage, L., and Moynihan, D. 2016. Yukon bedrock geology map. Yukon Geological Survey, Open File 2016-1, scale 1:1 000 000.

Cramer, B.D., and Saltzman, M.R. 2005. Sequestration of ^{12}C in the deep ocean during the early Wenlock (Silurian) positive carbon isotope excursion. Palaeogeography, Palaeoclimatology, Palaeoecology, **219**: 333–349. doi:10.1016/j.palaeo.2005.01.009.

Cramer, B.D., and Saltzman, M.R. 2007. Fluctuations in epeiric sea carbonate production during Silurian positive carbon isotope excursions: a review of proposed paleoceanographic models. Palaeogeography, Palaeoclimatology, Palaeoecology, **245**: 37–45. doi:10.1016/j.palaeo.2006.02.027.

Cramer, B.D., Kleffner, M.A., and Saltzman, M.R. 2006. The late Wenlock Mulde positive carbon isotope ($\delta^{13}C_{carb}$) excursion in North America. GFF, **128**: 85–90. doi:10.1080/11035890601282085.

Cramer, B.D., Brett, C.E., Melchin, M.J., Maennik, P., Kleffner, M.A., McLaughlin, P.I., et al. 2011. Revised correlation of Silurian Provincial Series of North America with global and regional chronostratigraphic units and $\delta^{13}C_{carb}$ chemostratigraphy. Lethaia, **44**: 185–202. doi:10.1111/j.1502-3931.2010.00234.x.

Crevello, P.D., and Schlager, W. 1980. Carbonate debris sheets and turbidites, Exuma Sound, Bahamas. Journal of Sedimentary Research, **50**: 1121–1147. doi:10.1306/212F7B99-2B24-11D7-8648000102C1865D.

Derby, J., Raine, R.J., Smith, M.P., and Runkel, A.C. 2012. Paleogeography of the Great American Carbonate Bank of Laurentia in the earliest Ordovician (Early Tremadocian): The Stonehenge Transgression. *Edited by* J.R. Derby, R.D. Fritz, S.A. Longacre, W.A. Morgan, and C.A. Sternbach. American Association of Petroleum Geologists Memoir, 98, pp. 649–673.

Dover, J.H. 1994. Geology of part of east-central Alaska. *In* The geology of Alaska. *Edited by* G. Plafker and H.C. Berg. Geological Society of America, Boulder, Colorado, G-1, pp. 153–204.

Dumoulin, J.A., and Harris, A.G. 2012. Cambrian–Ordovician sedimentary rocks of Alaska. *In* The Great American Carbonate Bank: the geology and economic resources of the Cambrian–Ordovician Sauk megasequence of Laurentia. *Edited by* J.R. Derby, R.D. Fritz, S.A. Longacre, W.A. Morgan, and C.A. Sternbach. American Association of Petroleum Geologists Memoir, 98, pp. 649–673.

Edwards, C.T., and Saltzman, M.R. 2014. Carbon isotope ($\delta^{13}C_{carb}$) stratigraphy of the Lower–Middle Ordovician (Tremadocian–Darriwilian) in the Great Basin, western United States: implications for global correlation. Palaeogeography, Palaeoclimatology, Palaeoecology, **399**: 1–20. doi:10.1016/j.palaeo.2014.02.005.

Edwards, C.T., and Saltzman, M.R. 2016. Paired carbon isotopic analysis of Ordovician bulk carbonate ($\delta^{13}C_{carb}$) and organic matter ($\delta^{13}C_{org}$) spanning the Great Ordovician Biodiversification Event. Palaeogeography, Palaeoclimatology, Palaeoecology, **458**: 102–117. doi:10.1016/j.palaeo.2015.08.005.

Edwards, C.T., Fike, D.A., Saltzman, M.R., Lu, W., and Lu, Z. 2018. Evidence for local and global redox conditions at an Early Ordovician (Tremadocian) mass extinction. Earth and Planetary Science Letters, **481**: 125–135. doi:10.1016/j.epsl.2017.10.002.

Erwin, D.H., Laflamme, M., Tweedt, S.M., Sperling, E.A., Pisani, D., and Peterson, K.J. 2011. The Cambrian conundrum: early divergence and later ecological success in the early history of animals. Science, **334**: 1091–1097. doi:10.1126/science.1206375. PMID:22116879.

Ferri, F., Rees, C., Nelson, J., and Legun, A. 1999. Geology and mineral deposits of the northern Kechika Trough between Gataga River and the 60th Parallel. Geological Survey Branch, Mineral Resources Division, British Columbia Ministry of Energy and Mines Bulletin, 107. 122pp.

Finnegan, S., Bergmann, K., Eiler, J.M., Jones, D.S., Fike, D.A., Eiseman, I., et al. 2011. The magnitude and duration of late Ordovician-early Silurian glaciation. Science, **331**: 903–906. doi:10.1126/science.1200803. PMID:21273448.

Fraser, T.A., and Hutchison, M.P. 2017. Lithogeochemical characterization of the Middle–Upper Devonian Road River Group and Canol and Imperial formations on Trail River, east Richardson Mountains, Yukon: age constraints and a depositional model for fine-grained strata in the Lower Paleozoic Richardson trough. Canadian Journal of Earth Sciences, **54**(17): 731–765. doi:10.1139/cjes-2016-0216.

Frýda, J., and Storch, P. 2014. Carbon isotope chemostratigraphy of the Llandovery in northern peri-Gondwana: new data from the Barrandian area, Czech Republic. Estonian Journal of Earth Sciences, **63**(4): 220–226. doi:10.3176/earth.2014.22.

Fritz, W.H. 1985. The basal contact of the Road River Group-a proposal for its location in the type area and in other selected areas in the Northern Canadian Cordillera. Current Research, Part B, Geological Survey of Canada, pp. 205–215. doi:10.4095/120246.

Fritz, W.H. 1997. Cambrian. *In* Geology and mineral and hydrocarbon potential of Northern Yukon territory and Northwestern district of Mackenzie. *Edited by* D.K. Norris. Geological Survey of Canada Bulletin, 422, pp. 85–117.

Fritz, W.H., Cecile, M.P., Norford, B.S., Morrow, D., and Geldsetzer, H.H.J. 1991. Cambrian to Middle Devonian Assemblages. *In* Geology of the Cordilleran Orogen in Canada. *Edited by* H. Gabrielse, and C.J. Yorath. Geological Survey of Canada, 4. pp. 151–218. doi:10.1130/DNAG-GNA-G2.151.

Frýda, J., and Manda, Š. 2013. A long-lasting steady period of isotopically heavy carbon in the late Silurian ocean: evolution of the $\delta^{13}C$ record and its significance for an integrated $\delta^{13}C$, graptolite and conodont stratigraphy. Bulletin of Geosciences, **88**: 463–482. doi:10.3140/bull.geosci.1436.

Gabrielse, H. 1963. McDame map area, Cassiar District, British Columbia. *In* Geological Survey of Canada Memoir, 319. 138pp.

Gabrielse, H. 1998. Geology of the Cry Lake and Dease Lake map areas, north-central British Columbia. Geological Survey of Canada Bulletin, **504**: 147. doi:10.4095/210074.

Gabrielse, H., Blusson, S.L., and Roddick, J.A. 1973. Geology of Flat River, Glacier Lake, and Wrigley Lake map areas, District of Mackenzie and Yukon Territory. Geological Survey of Canada Memoir, **366**: 153. doi:10.4095/100705.

Gadd, M.G., Peter, J.M., and Rogers, N. 2017. Field observations, mineralogy and geochemistry of Middle Devonian Ni-Zn-Mo-PGE hyper-enriched black shale deposits, Yukon. Geological Survey of Canada Targeted Geoscience Initiative, pp. 193–206.

Gadd, M.G., Peter, J.M., Jackson, S.E., Yang, Z., and Petts, D. 2019. Platinum, Pd, Mo, Au and Re deportment in hyper-enriched black shale Ni-Zn-Mo-PGE mineralization, Peel River, Yukon, Canada. Ore Geology Reviews, **107**: 600–614. doi:10.1016/j.oregeorev.2019.02.030.

Gadd, M.G., Peter, J.M., Hnatyshin, D., Creaser, R., Gouwy, S., and Fraser, T. 2020. A Middle Devonian basin-scale precious metal enrichment event across northern Yukon (Canada). Geology, **48**: 242–246. doi:10.1130/G46874.1.

Gill, B.C., Lyons, T.W., Young, S.A., Kump, L.R., Knoll, A.H., and Saltzman, M.R. 2011. Geochemical evidence for widespread euxinia in the later Cambrian ocean. Nature, **469**: 80–83. doi:10.1038/nature09700. PMID:21209662.

Goodfellow, W.D., Nowlan, G.S., McCracken, A.D., Lenz, A.C., and Grégoire, D.C. 1992. Geochemical anomalies near the Ordovician-Silurian boundary, Northern Yukon Territory, Canada. Historical Biology, **6**: 1–23. doi:10.1080/10292389209380415.

Goodfellow, W.D., Cecile, M.P., and Leybourne, M.I. 1995. Geochemistry, petrogenesis, and tectonic setting of lower Paleozoic alkalic and potassic volcanic rocks, Northern Canadian Cordilleran Miogeocline. Canadian Journal of Earth Sciences, **32**(8): 1236–1254. doi:10.1139/e95-101.

Goodfellow, W.D., Geldsetzer, H., Gregoire, C., Orchard, M., and Cordey, F. 2010. Geochemistry and origin of geographically extensive Ni (Mo, Zn, U)-PGE sulphide deposits hosted in Devonian black shales, Yukon [abs.]: geological Association of Canada, Cordilleran Section, TGI-3 Workshop. Public Geoscience in Support of Base Metal Exploration, pp. 15–18.

Gordey, S., and Anderson, R. 1993. Evolution of the Northern Cordilleran Miogeocline, Nahanni Map Area (105I), Yukon and Northwest Territories. Geological Survey of Canada Memoir, 428. 214pp. doi:10.4095/183983.

Gordey, S.P., and Roots, C.F. 2011. Chapter 2. Regional setting. *In* Geology of the central Mackenzie Mountains of the northern Canadian Cordillera, Sekwi Mountain (105P), Mount Eduni (106A), and northwestern Wrigley Lake (95M) map-areas, Northwest Territories. *Edited by* E. Martel, E.C. Turner, and B.J. Fischer. NWT Special Volume 1, NWT Geoscience Office, pp. 18–30.

Grammer, G.M., and Ginsburg, R.N. 1992. Highstand versus lowstand deposition on carbonate platform margins: insight from Quaternary foreslopes in the Bahamas. Marine Geology, **103**: 125–136. doi:10.1016/0025-3227(92)90012-7.

Grammer, G.M., Ginsburg, R.N., and Harris, P.M. 1993. Timing of Deposition, Diagenesis, and Failure of Steep Carbonate Slopes in Response to a High-Amplitude/High-Frequency Fluctuation in Sea Level, Tongue of the Ocean, Bahamas: Chapter 4. American Association of Petroleum Geologists Memoir, **168**: 107–131. doi:10.1306/M57579C4.

Hammarlund, E.U., Loydell, D.K., Nielsen, A.T., and Schovsbo, N.H. 2019. Early Silurian $\delta^{13}C_{org}$ excursions in the foreland basin of Baltica, both familiar and surprising. Palaeogeography, Palaeoclimatology, Palaeoecology, **526**: 126–135. doi:10.1016/j.palaeo.2019.03.035.

Harwood, G.M., and Towers, P.A. 1988, Seismic sedimentologic interpretation of a carbonate slope, north margin of Little Bahama Bank. *In* Proceedings of the Ocean Drilling Program, Scientific results, Volume 101: College Station, Texas, Ocean Drilling Program. *Edited by* J.A. Austin, Jr. et al. pp. 263–277. doi:10.2973/odp.proc.sr.101.143.1988.

Heim, N.A., Knope, M.L., Schaal, E.K., Wang, S.C., and Payne, J.L. 2015. Cope's rule in the evolution of marine animals. Science, **347**: 867–870. doi:10.1126/science.1260065. PMID:25700517.

Holmden, C., Mitchell, C.E., LaPorte, D.F., Patterson, W.P., Melchin, M.J., and Finney, S.C. 2013. Nd isotope records of late Ordovician sea-level change-Implications for glaciation frequency and global stratigraphic correlation. Palaeogeography, Palaeoclimatology, Palaeoecology, **386**: 131–144. doi:10.1016/j.palaeo.2013.05.014.

Horan, M.F., Morgan, J.W., Grauch, R.I., Coveney, R.M., Jr., Murowchick, J.B., and Hulbert, L.J. 1994. Rhenium and osmium isotopes in black shales and Ni-Mo-PGE-rich sulfide layers, Yukon Territory, Canada, and Hunan and Guizhou provinces, China. Geochimica et Cosmochimica Acta, **58**: 257–265. doi:10.1016/0016-7037(94)90463-4.

Hulbert, L.J., Gregoire, D.C., Paktunc, D., and Carne, R.C. 1992. Sedimentary nickel, zinc, and platinum-group-element mineralization in Devonian black shales at the Nick property, Yukon, Canada: a new deposit type. Exploration and Mining Geology, **1**: 39–62.

Husson, J.M., Schoene, B., Bluher, S., and Maloof, A.C. 2016. Chemostratigraphic and U–Pb geochronologic constraints on carbon cycling across the Silurian–Devonian boundary. Earth and Planetary Science Letters, **436**: 108–120. doi:10.1016/j.epsl.2015.11.044.

Innis, J.W. 1980. Sedimentology and stratigraphy of the Ordovician-Silurian Road River Formation, southern Richardson Mountains, Yukon Territory. M.Sc. thesis, the University of Western Ontario, London, Ontario.

Jackson, D.E., and Lenz, A.C. 1962. Zonation of Ordovician and Silurian Graptolites of Northern Yukon, Canada. AAPG Bulletin, **46**: 30–45. doi:10.1306/BC743757-16BE-11D7-8645000102C1865D.

Jackson, D.E., and Lenz, A.C. 2000. Some graptolites from the late Tremadoc and early Arenig of Yukon, Canada. Canadian Journal of Earth Sciences, **37**(8): 1177–1193.

Jackson, D.E., and Lenz, A.C. 2003. Taxonomic and biostratigraphical significance of the Tremadoc graptolite fauna from northern Yukon Territory, Canada. Geological Magazine, **140**: 131–156. doi:10.1017/S0016756802007227.

Jackson, D.E., and Lenz, A.C. 2006. The sequence and correlation of Early Ordovician (Arenig) graptolite faunas in the Richardson Trough and Misty Creek Embayment, Yukon Territory and District of Mackenzie, Canada. Canadian Journal of Earth Sciences, **43**(12): 1791–1820. doi:10.1139/e06-065.

Jarochowska, E., and Munnecke, A. 2016. Late Wenlock carbon isotope excursions and associated conodont fauna in the Podlasie Depression, eastern Poland: a not-so-big crisis? Geological Journal, **51**: 683–703. doi:10.1002/gj.2674.

Jeletzky, J.A. 1962. Pre-Cretaceous Richardson Mountains Trough-its place in tectonic framework of Arctic Canada and its bearing on some geosynclinal concepts. Transactions of the Royal Society of Canada, **56**: 55.

Jo, A., Eberli, G.P., and Grasmueck, M. 2015. Margin collapse and slope failure along southwestern Great Bahama Bank. Sedimentary Geology, **317**: 43–52. doi:10.1016/j.sedgeo.2014.09.004.

Johnson, C.A., Slack, J.F., Dumoulin, J.A., Kelley, K.D., and Falck, H. 2018. Sulfur isotopes of host strata for Howards Pass (Yukon–Northwest Territories) Zn-Pb deposits implicate anaerobic oxidation of methane, not basin stagnation. Geology, **46**: 619–622. doi:10.1130/G40274.1.

Kaljo, D., Grytsenko, V., Martma, T., and Mõtus, M.A. 2007. Three global carbon isotope shifts in the Silurian of Podolia (Ukraine): stratigraphical implications. Estonian Journal of Earth Sciences, **56**: 205–220. doi:10.3176/earth.2007.02.

LaPorte, D.F., Holmden, C., Patterson, W.P., Loxton, J.D., Melchin, M.J., Mitchell, C.E., et al. 2009. Local and global perspectives on carbon and nitrogen cycling during the Hirnantian glaciation. Palaeogeography, Palaeoclimatology, Palaeoecology, **276**: 182–195. doi:10.1016/j.palaeo.2009.03.009.

Lenz, A.C. 1968. Two new Lower Devonian atrypid brachiopods from Royal Creek, Yukon Territory, Canada. Journal of Paleontology, **42**(1): 180–185.

Lenz, A.C. 1972. Ordovician to Devonian history of Northern Yukon and adjacent district of Mackenzie. Bulletin of Canadian Petroleum Geology, **20**: 321–361. doi:10.35767/gscpgbull.20.2.321.

Lenz, A.C. 1978. Llandoverian and Wenlockian Cyrtograptus, and some other Wenlockian graptolites from Northern and Arctic Canada. Geobios, **11**: 623–653. doi:10.1016/S0016-6995(78)80003-5.

Lenz, A.C. 1982. New data on Late Silurian and Early Devonian brachiopods from the Royal Creek area, Yukon Territory. Canadian Journal of Earth Sciences, **19**(2): 364–375. doi:10.1139/e82-028.

Lenz, A.C. 1988. Upper Silurian and Lower Devonian graptolites and graptolite biostratigraphy, northern Yukon, Canada. Canadian Journal of Earth Sciences, **25**(3): 355–369. doi:10.1139/e88-039.

Lenz, A.C., and Jackson, D.E. 1986. Arenig and Llanvirn graptolite biostratigraphy, Canadian Cordillera. Geological Society, London, Special Publications, **20**: 27–45. doi:10.1144/GSL.SP.1986.020.01.05.

Lenz, A.C., and McCracken, A.D. 1982. The Ordovician–Silurian boundary, northern Canadian Cordillera: graptolite and conodont correlation. Canadian Journal of Earth Sciences, **19**(6): 1308–1322. doi:10.1139/e82-111.

Lenz, A.C., and Pedder, A.E.H. 1972. Lower and Middle Paleozoic Sediments and Paleontology of Royal Creek and Peel River, Yukon, and Powell Creek, NWT. *In* 24th International Geological Congress. Excursion A-14.

Lenz, A.C., and Xu, C. 1985. Middle to Upper Ordovician graptolite biostratigraphy of Peel River and other areas of the northern Canadian Cordillera. Canadian Journal of Earth Sciences, **22**(2): 227–239. doi:10.1139/e85-020.

Li, D., Zhang, X., Chen, K., Zhang, G., Chen, X., Huang, W., Peng, S., and Shen, Y. 2017. High-resolution C-isotope chemostratigraphy of the uppermost Cambrian stage (Stage 10) in South China: implications for defining the base of Stage 10 and palaeoenvironmental change. Geological Magazine, **154**: 1232–1243. doi:10.1017/S0016756817000188.

Lowe, D.R. 1982. Sediment gravity flows; II, Depositional models with special reference to the deposits of high-density turbidity currents. Journal of Sedimentary Research, **52**: 279–297. doi:10.1306/212F7F31-2B24-11D7-8648000102C1865D.

Lowe, D.R. 1988. Suspended-load fallout rate as an independent variable in the analysis of current structures. Sedimentology, **35**: 765–776. doi:10.1111/j.1365-3091.1988.tb01250.x.

Loxton, J.D. 2017. Graptolite diversity, and community changes surrounding the late Ordovician mass extinction: high resolution data from the Blackstone River, Yukon. Unpublished Ph.D. thesis, Dalhousie University, Halifax, N.S., Canada. 590pp.

Ludvigsen, R. 1975. Ordovician Formations and Faunas, Southern Mackenzie Mountains. Canadian Journal of Earth Sciences, **12**(4): 663–697. doi:10.1139/e75-059.

Ludvigsen, R. 1982. Upper Cambrian and Lower Ordovician trilobite biostratigraphy of the Rabbitkettle Formation, western District of Mackenzie. Royal Ontario Museum, Life Sciences Contribution, **14**. doi:10.5962/bhl.title.52077.

Ludvigson, G.A., Witzke, B.J., González, L.A., Carpenter, S.J., Schneider, C.L., and Hasiuk, F. 2004. Late Ordovician (Turinian–Chatfieldian) carbon isotope excursions and their stratigraphic and paleoceanographic significance. Palaeogeography, Palaeoclimatology, Palaeoecology, **210**: 187–214. doi:10.1016/j.palaeo.2004.02.043.

Lynts, G.W., Judd, J.B., and Stehman, C.F. 1973. Late Pleistocene History of Tongue of the Ocean, Bahamas. GSA Bulletin, **84**: 2665–2684. doi:10.1130/0016-7606(1973)84<2665:LPHOTO>2.0.CO;2.

MacNaughton, R.B., and Fallas, K.M. 2014. Nainlin Formation, a new Middle Cambrian map unit from the Mackenzie Mountains, Northwest Territories. Bulletin of Canadian Petroleum Geology, **62**: 37–67. doi:10.2113/gscpgbull.62.2.37.

MacNaughton, R.B., Pratt, B.R., and Fallas, K.M. 2013. Observations on Cambrian stratigraphy in the eastern Mackenzie Mountains, Northwest Territories. Geological Survey of Canada Current Research, **10**: 11. doi:10.4095/292423.

MacNaughton, R.B., Moynihan, D.P., Roots, C.F., and Crowley, J.L. 2016. New occurrences of Oldhamia in eastern Yukon, Canada: stratigraphic context and implications for Cambrian deep-marine biostratigraphy. Ichnos, **23**: 33–52. doi:10.1080/10420940.2015.1127232.

McAdams, N.E., Cramer, B.D., Bancroft, A.M., Melchin, M.J., Devera, J.A., and Day, J.E. 2019. Integrated $\delta^{13}C_{carb}$, conodont, and graptolite biochemostratigraphy of the Silurian from the Illinois Basin and stratigraphic revision of the Bainbridge Group. Geological Society of America Bulletin, **131**: 335–352. doi:10.1130/B32033.1.

McCracken, A.D., and Lenz, A.C. 1987. Middle and Late Ordovician conodont faunas and biostratigraphy of graptolitic strata of the Road River Group, northern Yukon Territory. Canadian Journal of Earth Sciences, **24**(4): 643–653. doi:10.1139/e87-062.

Melchin, M.J., and Holmden, C. 2006. Carbon isotope chemostratigraphy of the Llandovery in Arctic Canada: implications for global correlation and sea-level change. GFF, **128**: 173–180. doi:10.1080/11035890601282173.

Melchin, M.J., Sadler, P.M., Cramer, B.D., Cooper, R.A., Gradstein, F.M., and Hammer, O. 2012. The Silurian Period. *In* The geologic time scale 2012, Vol. 2. *Edited by* F.M. Gradstein, J.G. Ogg, M. Schmitz, and G. Ogg. Elsevier BV, Amsterdam, the Netherlands. pp. 525–558.

Melchin, M.J., Mitchell, C.E., Holmden, C., and Štorch, P. 2013. Environmental changes in the Late Ordovician–early Silurian: review and new insights from black shales and nitrogen isotopes. Geological Society of America Bulletin, **125**: 1635–1670. doi:10.1130/B30812.1.

Melchin, M.J., MacRae, K.D., and Bullock, P. 2015. A multi-peak organic carbon isotope excursion in the late Aeronian (Llandovery, Silurian): evidence from Arisaig, Nova Scotia, Canada. Palaeoworld, **24**: 191–197. doi:10.1016/j.palwor.2014.12.004.

Miller, J.F. 2019. Study and Use of Upper Cambrian to Lower Ordovician conodonts in central, southern, and western Laurentia, 1933–2018. Palaeobiodiversity and Palaeoenvironments, **100**: 95–133. doi:10.1007/s12549-019-00380-9.

Mohrig, D., Ellis, C., Parker, G., Whipple, K.X., and Hondzo, M. 1998. Hydroplaning of subaqueous debris flows. GSA Bulletin, **110**: 387–394. doi:10.1130/0016-7606(1998)110<0387:HOSDF>2.3.CO;2.

Morrow, D.W. 1999. Lower Paleozoic stratigraphy of northern Yukon Territory and northwestern District of Mackenzie. Geological Survey of Canada Bulletin, 538. doi:10.4095/210998.

Moynihan, D.P., Strauss, J.V., Nelson, L.L., and Padget, C.D. 2019. Upper Windermere Supergroup and the transition from rifting to continent-margin sedimentation, Nadaleen River area, northern Canadian Cordillera. GSA Bulletin, **131**: 1673–1701. doi:10.1130/B32039.1.

Mulder, T., and Alexander, J. 2001. Abrupt change in slope causes variation in the deposit thickness of concentrated particle-driven density currents. Marine Geology, **175**: 221–235. doi:10.1016/S0025-3227(01)00114-1.

Mulder, T., Ducassou, E., Gillet, H., Hanquiez, V., Tournadour, E., Combes, J., et al. 2012. Canyon morphology on a modern carbonate slope of the Bahamas: evidence of regional tectonic tilting. Geology, **40**: 771–774. doi:10.1130/G33327.1.

Mulder, T., Ducassou, E., Gillet, H., Hanquiez, V., Principaud, M., Chabaud, L., et al. 2014. First discovery of channel–levee complexes in a modern deep-water carbonate slope environment. Journal of Sedimentary Research, **84**: 1139–1146. doi:10.2110/jsr.2014.90.

Mullins, H.T., Dolan, J., Breen, N., Andersen, B., Gaylord, M., Petruccione, J.L., et al. 1991. Retreat of carbonate platforms: response to tectonic processes. Geology, **19**: 1089–1092. doi:10.1130/0091-7613(1991)019<1089:ROCPRT>2.3.CO;2.

Munnecke, A., Samtleben, C., and Bickert, T. 2003. The Ireviken Event in the lower Silurian of Gotland, Sweden–relation to similar Palaeozoic and Proterozoic events. Palaeogeography, Palaeoclimatology, Palaeoecology, **195**: 99–124. doi:10.1016/S0031-0182(03)00304-3.

Murphy, D.C. 2018. Latest Cretaceous–early Eocene Pacific-Arctic?-Atlantic connection: co-evolution of strike-slip fault systems, oroclines, and transverse fold-and-thrust belts in the northwestern North American Cordillera. *In* Circum-Arctic Structural Events: tectonic Evolution of the Arctic Margins and Trans-Arctic Links with Adjacent Orogens. *Edited by* K. Piepjohn, J.V. Strauss, L. Reinhardt, and W.C. McClelland. Geological Society of America Special Paper, 541. doi:10.1130/2018.2541(28).

Nelson, J.L., Colpron, M., and Israel, S. 2013. The Cordillera of British Columbia, Yukon, and Alaska: tectonics and Metallogeny. *In* Tectonics, metallogeny, and discovery: the North American Cordillera and similar accretionary settings. *Edited by* M. Colpron, T. Bissing, B.G. Rusk, and J.F.H. Thompson, Society of Economic Geologists Special Publication, 58, pp. 53–109.

Norford, B.S. 1964. Reconnaissance of the Ordovician and Silurian rocks of northern Yukon Territory. Geological Survey of Canada Paper, 63.

Norford, B.S. 1997. Ordovician and Silurian. *In* The geology, mineral and hydrocarbon potential of northern Yukon Territory and northwestern District of Mackenzie. *Edited by* D.K. Norris. Geological Survey of Canada Bulletin, 422, pp. 119–162.

Norris, D.K. 1981*a*. Geology, Eagle River, Yukon Territory. Geological Survey of Canada, Map 1523A. 1:250 000 scale.

Norris, D.K. 1981*b*. Geology, Trail River, Yukon Territory. Geological Survey of Canada, Map 1524A. 1:250 000 scale.

Norris, D.K. 1981*c*. Geology, Ogilvie River, Yukon Territory. Geological Survey of Canada, Map 1526A. 1:250 000 scale.

Norris, D.K. 1982*a*. Geology, Hart River, Yukon Territory. Geological Survey of Canada, Map 1527A. 1:250 000 scale.

Norris, D.K. 1982*b*. Geology, Wind River, Yukon Territory. Geological Survey of Canada, Map 1528A. 1:250 000 scale.

Norris, D.K. 1997. The geology, mineral and hydrocarbon potential of northern Yukon Territory and northwestern District of Mackenzie. Geological Survey of Canada Bulletin, 422. doi:10.4095/208886.

Nowlan, G.S. 2019. Report on twenty-one samples from the Peel Canyon section (collectors Tyler Allen and Tiffani Fraser) and the Nadaleen Mountain section (collector Justin Strauss), Yukon; Fire Bay, Ellesmere Island, Nunavut (collector Justin Strauss) and samples from the Day and Megunticook formations, Maine, US.A. submitted by Justin Strauss (Dartmouth College) for conodont analysis. NTS 106C/06, 106E/l3, 560D/08. Geological Survey of Canada, Paleontological Report 001-GSN-2019. 9pp.

Pages, A., Barnes, S., Schmid, S., Coveney, R.M., Jr., Schwark, L., Liu, W., et al. 2018. Geochemical investigation of the lower Cambrian mineralised black shales of South China and the late Devonian Nick deposit, Canada. Ore Geology Reviews, **94**: 396–413. doi:10.1016/j.oregeorev.2018.02.004.

Payne, M.W., and Allison, C.W. 1981. Paleozoic continental-margin sedimentation in east-central Alaska. Geology, **9**: 274–279. doi:10.1130/0091-7613(1981)9<274:PCSIEA>2.0.CO;2.

Peng, S., Babcock, L., Robison, R., Lin, H., Rees, M., and Saltzman, M. 2004. Global Standard Stratotype-section and Point (GSSP) of the Furongian Series and Paibian Stage (Cambrian). Lethaia, **37**: 365–379. doi:10.1080/00241160410002081.

Pigage, L.C., Roots, C.F., and Abbott, J.G. 2015. Regional bedrock geology for the Coal River map area (NTS 95D), southeast Yukon. Yukon Geological Survey Bulletin, 17. 155pp.

Pilskaln, C.H., Neumann, A.C., and Bane, J.M. 1989. Periplatform carbonate flux in the northern Bahamas. Deep Sea Research Part A, Oceanographic Research Papers, **36**: 1391–1406. doi:10.1016/0198-0149(89)90090-3.

Post, R.T., and Long, D.G.F. 2008. The Middle Cambrian Mount Roosevelt Formation (new) of northeastern British Columbia: evidence for rifting and development of the Kechika Graben System. Canadian Journal of Earth Sciences, **45**(4): 483–498. doi:10.1139/E08-014.

Pratt, B.R. 1988. An Ibexian (Early Ordovician) trilobite faunule from the type section of the Rabbitkettle Formation (southern Mackenzie Mountains, Northwest Territories). Canadian Journal of Earth Sciences, **25**(10): 1595–1607. doi:10.1139/e88-152.

Pratt, B.R. 1992. Trilobites of the Marjuman and Steptoean stages (Upper Cambrian), Rabbitkettle Formation, southern Mackenzie Mountains, northwest Canada. Palaeontographica Canadiana 9.

Pugh, D.C. 1983. Pre-Mesozoic geology in the subsurface of Peel River map area, Yukon Territory and District of Mackenzie. Geological Survey of Canada Memoir, 401.

Pyle, L.J. 2012. Cambrian and Lower Ordovician Sauk Megasequence of Northwestern Canada, Northern Rocky Mountains to the Beaufort Sea. *In* The Great American Carbonate Bank: the geology and economic resources of the Cambrian–Ordovician Sauk megasequence of Laurentia. *Edited by* J.R. Derby, R.D. Fritz, S.A. Longacre, W.A. Morgan, and C.A. Sternbach. American Association of Petroleum Geologists Memoir, 98. pp. 675–723.

Pyle, L.J., and Barnes, C.R. 2000. Upper Cambrian to Lower Silurian stratigraphic framework of platform-to-basin facies, northeastern British Columbia. Bulletin of Canadian Petroleum Geology, **48**: 123–149. doi:10.2113/48.2.123.

Pyle, L.J., and Barnes, C.R. 2001. Conodonts from the Kechika Formation and Road River Group (Lower to Upper Ordovician) of the Cassiar Terrane, northern British Columbia. Canadian Journal of Earth Sciences, **38**(10): 1387–1401. doi:10.1139/e01-033.

Pyle, L.J., and Barnes, C.R. 2003. Lower Paleozoic stratigraphic and biostratigraphic correlations in the Canadian Cordillera: implications for the tectonic evolution of the Laurentian margin. Canadian Journal of Earth Sciences, **40**(12): 1739–1753. doi:10.1139/e03-049.

Pyle, L.J., Orchard, M.J., Barnes, C.R., and Landry, M.L. 2003. Conodont biostratigraphy of the Lower to Middle Devonian Deserters Formation (new), Road River Group, northeastern British Columbia. Canadian Journal of Earth Sciences, **40**(1): 99–113. doi:10.1139/e02-095.

Rasmussen, C.M.Ø., Kröger, B., Nielsen, M.L., and Colmenar, J. 2019. Cascading trend of Early Paleozoic marine radiations paused by Late Ordovician extinctions. Proceedings of the National Academy of Sciences, **116**: 7207–7213. doi:10.1073/pnas.1821123116.

Read, J.F. 1982. Carbonate platforms of passive (extensional) continental margins: types, characteristics and evolution. Tectonophysics, **81**: 195–212. doi:10.1016/0040-1951(82)90129-9.

Read, J.F. 1985. Carbonate platform facies models. American Association of Petroleum Geologists Bulletin, **69**: 1–21. doi:10.1306/AD461B79-16F7-11D7-8645000102C1865D.

Rigby, J.K., Potter, A.W., and Blodgett, R.B. 1988. Ordovician sphinctozoan sponges of Alaska and Yukon Territory. Journal of Paleontology, **62**: 731–746.

Roots, C.F. 1988. Cambro-Ordovician volcanic rocks in the eastern Dawson map area, Ogilvie mountains, Yukon. *In* Yukon geology. Vol. 2. *Edited by* G. Abbott. Indian and Northern Affairs Canada, Geology Section, Whitehorse, Yukon, pp. 81–87.

Saltzman, M.R. 2002. Carbon isotope ($\delta^{13}C$) stratigraphy across the Silurian–Devonian transition in North America: evidence for a perturbation of the global carbon cycle. Palaeogeography, Palaeoclimatology, Palaeoecology, **187**: 83–100. doi:10.1016/S0031-0182(02)00510-2.

Saltzman, M.R. 2005. Phosphorus, nitrogen, and the redox evolution of the Paleozoic oceans. Geology, **33**: 573–576. doi:10.1130/G21535.1.

Saltzman, M.R., and Thomas, E. 2012. Carbon isotope stratigraphy. *In* The geologic time scale. Vol. 2. *Edited by* F.M. Gradstein, J.G. Ogg, M. Schmitz, and G. Ogg. Elsevier BV, Amsterdam, the Netherlands, pp. 207–232. doi:10.1016/B978-0-444-59425-9.00011-1.

Saltzman, M.R., Ripperdan, R.L., Brasier, M.D., Lohmann, K.C., Robison, R.A., Chang, W.T., et al. 2000. A global carbon isotope excursion (SPICE) during the Late Cambrian: relation to trilobite extinctions, organic-matter burial and sea level. Palaeogeography, Palaeoclimatology, Palaeoecology, **162**: 211–223. doi:10.1016/S0031-0182(00)00128-0.

Saltzman, M.R., Cowan, C.A., Runkel, A.C., Runnegar, B., Stewart, M.C., and Palmer, A.R. 2004. The Late Cambrian Spice ($\delta^{13}C$) Event and the Sauk II-Sauk III Regression: new Evidence from Laurentian Basins in Utah, Iowa, and Newfoundland. Journal of Sedimentary Research, **74**: 366–377. doi:10.1306/120203740366.

Saltzman, M.R., Young, S.A., Kump, L.R., Gill, B.C., Lyons, T.W., and Runnegar, B. 2011. Pulse of atmospheric oxygen during the late Cambrian. Proceedings of the National Academy of Sciences, **108**: 3876–3881. doi:10.1073/pnas.1011836108.

Saltzman, M.R., Edwards, C.T., Adrain, J.M., and Westrop, S.R. 2015. Persistent oceanic anoxia and elevated extinction rates separate the Cambrian and Ordovician radiations. Geology, **43**: 807–810. doi:10.1130/G36814.1.

Schlager, W., and Chermak, A. 1979. Sediment facies of platform-basin transition, Tongue of the Ocean, Bahamas. Soceity of Economic Paleontologists and Mineralogists Special Publication, **27**: 193–208. doi:10.2110/pec.79.27.0193.

Scorrer, S., Azmy, K., and Stouge, S. 2019. Carbon-isotope stratigraphy of the Furongian Berry Head Formation (Port au Port Group) and Tremadocian Watts Bight Formation (St. George Group), western Newfoundland, and the correlative significance. Canadian Journal of Earth Sciences, **56**(3): 223–234. doi:10.1139/cjes-2018-0059.

Servais, T., Lehnert, O., Li, J., Mullins, G.L., Munnecke, A., Nützel, A., and Vecoli, M. 2008. The Ordovician biodiversification: revolution in the oceanic trophic chain. Lethaia, **41**: 99–109. doi:10.1111/j.1502-3931.2008.00115.x.

Slack, J.F., Falck, H., Kelley, K.D., and Xue, G.G. 2017. Geochemistry of host rocks in the Howards Pass district, Yukon-Northwest Territories, Canada: implications for sedimentary environments of Zn-Pb and phosphate mineralization. Mineralium Deposita, **52**: 565–593. doi:10.1007/s00126-016-0680-x.

Sloss, L.L. 1963. Sequences in the Cratonic Interior of North America. Geological Society of America Bulletin, **74**: 93–114. doi:10.1130/0016-7606(1963)74[93:SITCIO]2.0.CO;2.

Smith, R.E. 1980. Lower Devonian (Lochkovian) biostratigraphy and brachiopod faunas, Canadian Arctic Islands: Geological Survey of Canada, Bulletin, 308.

Spence, G.H., and Tucker, M.E. 1997. Genesis of limestone megabreccias and their significance in carbonate sequence stratigraphic models: a review. Sedimentary Geology, **112**: 163–193. doi:10.1016/S0037-0738(97)00036-5.

Strauss, J.V., Macdonald, F.A., Halverson, G.P., Tosca, N.J., Schrag, D.P., and Knoll, A.H. 2015. Stratigraphic evolution of the Neoproterozoic Callison Lake Formation: linking the break-up of Rodinia to the Islay carbon isotope excursion. American Journal of Science, **315**: 881–944. doi:10.2475/10.2015.01.

Taylor, J.F., Repetski, J.E., Loch, J.D., and Leslie, S.A. 2012. Biostratigraphy and Chronostratigraphy of the Cambrian–Ordovician Great American Carbonate Bank. *In* The Great American Carbonate Bank: the geology and economic resources of the Cambrian–Ordovician Sauk megasequence of Laurentia. *Edited by* J.R. Derby, R.D. Fritz, S.A. Longacre, W.A. Morgan, and C.A. Sternbach. American Association of Petroleum Geologists Memoir, 98. pp. 1–21.

Taylor, J.F., Allen, T.J., Repetski, J.E., Strauss, J.V., and Irwin, S.J. 2015. Life on the edge in eastern Alaska: basal Ordovician (Tremadocian) platform-margin faunas of the Jones Ridge Limestone. *In* 12th International Symposium on the Ordovician System, Short Papers and Abstracts: Stratigraphy, vol. 12, no. 2. *Edited by* S.A. Leslie, D. Goldman, and R.C. Orndorff, pp. 70–77.

von Gosen, W., Piepjohn, K., McClelland, W.C., and Colpron, M. 2019. Evidence for the sinistral Porcupine shear zone in North Yukon (Canadian Arctic) and geotectonic implications. *In* Circum-Arctic Structural Events: tectonic Evolution of the Arctic Margins and Trans-Arctic Links with Adjacent Orogens. *Edited by* K. Piepjohn, J.V. Strauss, L. Reinhardt, and W.C. McClelland. Geological Society of America Special Paper, 541.

Wang, X.-F., Stouge, S., Maletz, J., Bagnoli, G., Qi, Y.-P., Raevskaya, E.G., Wang, C.-S., and Yan, C.-B. 2019. Correlating the global Cambrian–Ordovician boundary: precise comparison of the Xiaoyangqiao section, Dayangcha, North China with the Green Point GSSP section, Newfoundland, Canada. Palaeoworld, **28**: 243–275. doi:10.1016/j.palwor.2019.01.003.

Wilber, R.J., Milliman, J.D., and Halley, R.B. 1990. Accumulation of bank-top sediment on the western slope of Great Bahama Bank: rapid progradation of a carbonate megabank. Geology, **18**: 970–974. doi:10.1130/0091-7613(1990)018<0970:AOBTSO>2.3.CO;2.

Young, S.A., Saltzman, M.R., and Bergström, S.M. 2005. Upper Ordovician (Mohawkian) carbon isotope ($\delta^{13}C$) stratigraphy in eastern and central North America: regional expression of a perturbation of the global carbon cycle. Palaeogeography, Palaeoclimatology, Palaeoecology, **222**: 53–76. doi:10.1016/j.palaeo.2005.03.008.